1967

A study of the afterglow of an R-F excited mercury discharge

James A. Aubrecht

A STUDY OF THE AFTERGLOW OF AN R-F EXCITED MERCURY DISCHARGE

BY

JAMES A. AUBRECHT -1944-

AN

ABSTRACT

submitted to the faculty of

THE UNIVERSITY OF MISSOURI AT ROLLA

in partial fulfillment of the requirements for the

Degree of

MASTER OF SCIENCE IN PHYSICS

Rolla, Missouri

1967

Approved by

Richard Anderson (Advisor) Richard D. Rechtien

Fred C. Hamble, Jr. Robert J. Bell

ABSTRACT

The short duration afterglow of an r-f discharge in mercury has been examined versus ground state mercury atom density and r-f power. The intensity of the 5771, 5462, 4360, 4079, 4047, 3907, 3651/56, 3342, and 3127/32Å atomic mercury lines were observed to decay as a function of time after the shut off of the active discharge. At temperatures below 333°K, all atomic lines decayed exponentially, and no molecular emission was observed. From 333°K to 423°K, the atomic lines were observed to decay rapidly initially, then exhibit an enhancement effect in intensity which was produced by metastable atom collisions, and finally, the intensity decayed with a small time constant. Above 433°K, molecular emission begins to become effective because of the increased ground state atom density, and the overall intensity of the atomic lines is observe to decrease, but the intensity of the lines still exhibited an enhancement effect. Above 473°K, molecular emission becomes dominate, and the molecular emission robs the atomic line spectra of energy. From the comparison of theory and result of the experiment, the coefficient of ambipolar diffusion (D_e) for the electron can be calculated. The average value calculated is $D_e = 991$ cm^2/sec. Also, the average value of the lifetime of the metastable 6^3P_2 state of mercury can be calculated $T_m = 47$ microseconds.

A STUDY OF THE AFTERGLOW OF AN R-F EXCITED MERCURY DISCHARGE

BY

JAMES A. AUBRECHT

A

THESIS

submitted to the faculty of

THE UNIVERSITY OF MISSOURI AT ROLLA

in partial fulfillment of the requirements for the

Degree of

MASTER OF SCIENCE IN PHYSICS

Rolla, Missouri

1967

Approved by

(Advisor)

ACKNOWLEDGMENTS

The author wishes to acknowledge the assistance of the staff of the Physics Department of the University of Missouri at Rolla. In particular he would like to thank Dr. Richard Anderson and Mr. Robert Pickett for their help and direction. The author wishes also to acknowledge Mr. Victor Pol for the computer program that was used in the analysis of the results.

TABLE OF CONTENTS

LIST OF FIGURES

LIST OF TABLES

I. INTRODUCTION

A. REVIEW OF LITERATURE

Soon after the discovery of x-rays by Roentgen, the property of x-rays to cause a non-conducting gas to conduct was put to experimental use. Ionization of gas molecules by x-rays became a tool by which Rutherford,[1] studied the recombination of gases. J. Sayer[2] used a method similar to Rutherford's ionized air molecules. His ionization chamber was a cylindrical pyrex envelope with metal electrodes. The air was ionized by x-rays and secondary electrons were ejected from the gas molecules. These electrons were then captured by neutral oxygen molecules before they could recombine with a positive ion. This recombination with neutral 0_2 molecules yielded positive and negative ion concentrations in the tube. These concentrations could be measured by applying a high voltage pulse to the electrodes. In order to set up the rate equations for the decay of the ions in this experiment, it is assumed that equal positive and negative ions are created with random distributions and also that neutralization occurs only upon collision of positive and negative ions. Under these assumptions, the rate equation would be $\frac{dn}{dt} = \alpha n^2$, for the removal of ions after removal of the ionizing x-rays.

The above experiment was a crude beginning to the study of ion-ion and electron-ion recombination. Afterglow experiments have been performed using numerous techniques and gases. Those of particular interest are the afterglow experiments performed on mercury. Experimental studies of electron-ion recombination have used several techniques;[3,4,5,6,7] spectroscopic observation of the light intensity and microwave and probe techniques to measure the electron

density as a function of time. Also, pulsed electric discharges have been used for ionization of sample gases. Microwave techniques are used for the ionization of the sample gas, and they are also used to measure the electron density. The resulting change in frequency of the microwave cavity is a measure of the electron density:

$$\frac{\Delta f}{f} = \frac{1}{2} \frac{\bar{n}}{(1 + \frac{\nu}{\omega}) n_p} \qquad (1)$$

where $\bar{n}$ is the average electron density, ν is the electron collision frequency, ω is the angular frequency of the probing signal; $n_p = m_e \frac{\omega_p^2}{e^2}$, where ω_p in this term is the plasma resonance frequency, m_e is the mass of the electron, and e − is the charge of the electron.

B. EXPERIMENTAL STUDIES ON MERCURY

M. A. Biondi[6] used microwave measurements to determine the atomic processes causing the electron removal in a mercury afterglow. In his work, he suggested ambipolar diffusion as a loss mechanism for the electron at low pressure in the afterglow. Also, a production mechanism was suggested for the electrons due to collisions of metastable atoms:

$$\text{(a)}\quad Hg^*_m + Hg^*_m \rightarrow Hg^* + e^- + Hg.$$

If the electrons are produced by metastable atom collisions and are lost by ambipolar diffusion, Biondi said the electron density obeyed the following equation:

$$n_e = A\exp(-t/T_D) - B\exp(-2t/T_m),$$

where n_e is the electron density, T_D is the characteristic ambipolar diffusion

length, T_m is the lifetime of the metastable state, and A and B are independent of time. Because their diffusion coefficient is much larger than that of the ions, the electrons try to diffuse more rapidly than the ions toward regions of lower concentration. The electron motion is impeded because of the space charge field created due to the electron-ion separation, thus slowing down the diffusion of the electron and increasing the diffusion of the ion. This type of diffusion is called ambipolar diffusion.

At high pressure or atom densities, mercury band structure begins to enter the picture. A. O. McCoubrey[8] studied the band fluorescence of an optically excited mercury vapor during the afterglow. The experimental results led to an interpretation that the optically excited $Hg^*(6^3P_1)$ atoms are converted into metastable Hg^*_m (6^3P_0) atoms by collisions with ground state atoms.

The $Hg^*_m(6^3P_0)$ atoms are then converted into metastable $Hg^*_{2m}(^3O_u^-)$ molecules by a three body collision.

$$(b)\ Hg^*_m(6^3P_0^-) + 2Hg \rightarrow Hg^*_{2m}(^3O_u^-) + Hg$$

$$(c)\ Hg^*_{2m}(^3O_u^-) \rightarrow Hg_2 + h\nu(3350\text{Å})$$

$$(d)\ Hg^*_{2m}(^3O_u^-) + 2Hg + h\nu(4850\text{Å}).$$

The $Hg^*_{2m}(^3O_u^-)$ molecule decays by the emission of two band systems at 3350Å and 4850Å.

In a theoretical paper by W. H. Kunkel,[9] the differential equations governing the removal of ions and electrons from the afterglow for any generalized gas have been solved for three special cases. Ion production methods were introduced involving metastable atoms in two of these cases.

Since the metastable mercury atoms play an important role in the after-

glow of a discharge, several studies have been performed concerning the role of metastable atoms in the afterglow of mercury. Absorption studies involving metastable atoms $Hg^*(6^3P_{0,2})$ in a mercury-argon discharge have been performed by C. Kenty[10] and M. Yokoyama[11]. The results of these experiments give the relative population densities of the metastable states and the resonance state, $Hg^*(6^3P_1)$ versus time. From this information, fractional absorptions and apparent lifetimes of these states in the afterglow under various conditions can be determined.

II. THEORY

A. THE MECHANISM PRODUCING THE AFTERGLOW SPECTRA

The explanation of the atomic and molecular emission in the afterglow of a mercury discharge is a complicated problem because of the many processes involved. In the following experiment, a study of the intensity of the atomic emission lines of mercury as a function of time and atom density was performed. The intensity behavior of the atomic spectral lines, after the removal of the r-f exciting source, showed a rapid decrease in intensity for temperatures below $333^{o}K$. This decay was a simple exponential. Above $333^{o}K$ and below $433^{o}K$, the intensity showed an initial rapid decay, followed by an increase in intensity, and then a slow decrease in intensity towards zero. Above $433^{o}K$, the intensity initially increased or enhanced and this was followed by a slow decrease towards zero intensity. There are three temperature regions for which the data must be explained. The temperature and atom density will be used interchangeably to describe a certain region of the data because in this experiment the atom density of mercury is uniquely determined by the temperature of the cell. Therefore, a low temperature implies a low atom density.

Several possible mechanisms such as electron-ion recombination, electron production by ionizing collisions between metastable atoms, and natural radiative decay will be employed to explain the afterglow results. Some of the mechanisms producing the observed atomic line afterglow spectrum are:

(e) $Hg^{*} \rightarrow Hg + h\nu$

(f) $Hg^{*}_{m}(6^{3}P_{2}) + Hg^{*}_{m}(6^{3}P_{2}) \rightarrow Hg^{+} + e^{-} + Hg$

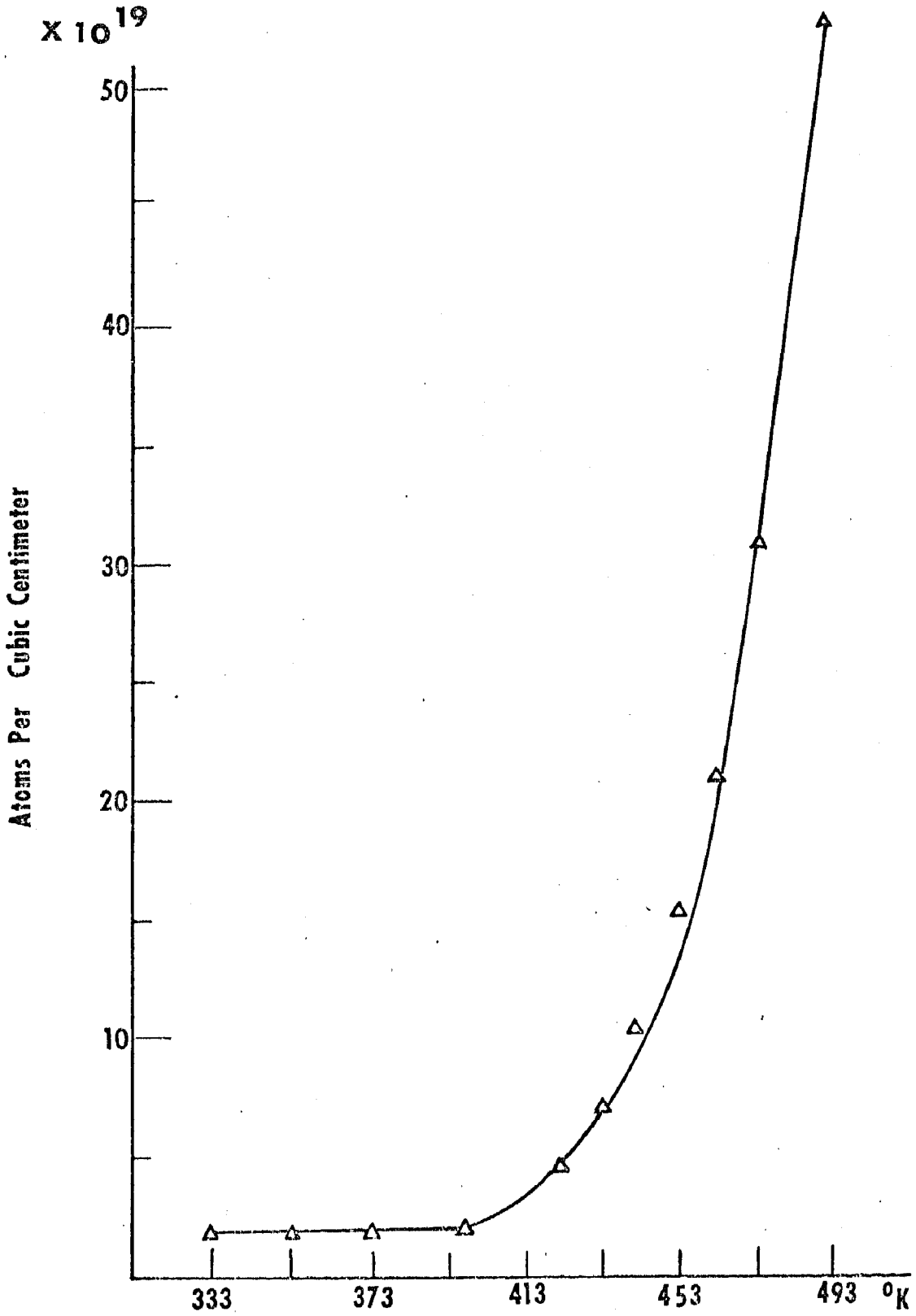

Figure 1. Atom density versus temperature.

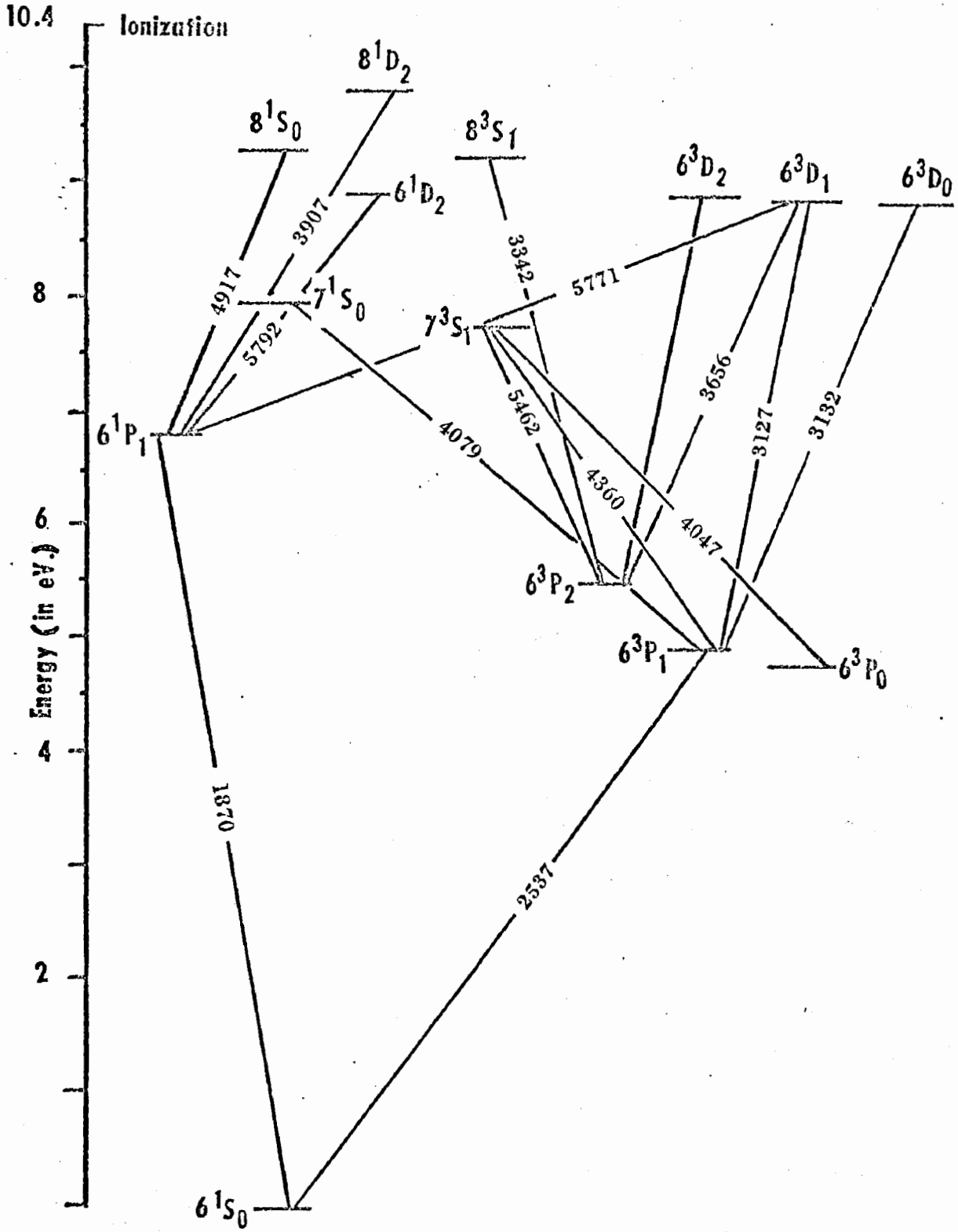

Figure 2. Energy level diagram of mercury.

$$Hg^*(6^1P_1) + Hg^*(6^1P_1) \rightarrow Hg^+ + e^- + Hg$$

$$Hg^*(6^1P_1) + Hg_m^*(6^3P_2) \rightarrow Hg^+ + e^- + Hg$$

$$Hg^*(6^1P_1) + Hg^*(6^3P_1) \rightarrow Hg^+ + e^- + Hg$$

$$Hg^*(6^1P_1) + Hg_m^*(6^3P_0) \rightarrow Hg^+ + e^- + Hg$$

(g) $$Hg^+ + e^- \rightarrow Hg^* \rightarrow Hg + h\nu$$

(h) $$Hg_m^*(6^3P_0) + Hg_m^*(6^3P_0) \rightarrow Hg^* + Hg \rightarrow 2Hg + h\nu$$

$$Hg^*(6^3P_1) + Hg^*(6^3P_1) \rightarrow Hg^* + Hg \rightarrow 2Hg + h\nu$$

$$Hg^*(6^3P_1) + Hg^*(6^3P_0) \rightarrow Hg^* + Hg \rightarrow 2Hg + h\nu$$

$$Hg^*(6^3P_1) + Hg_m^*(6^3P_2) \rightarrow Hg^* + Hg \rightarrow 2Hg + h\nu.$$

Equation (e) is the reaction for natural atomic photon emission, equations (f) are the reactions for electron production due to ionization by metastable and imprisoned atom collisions, equation (g) is the reaction for producing excited atomic states of mercury atoms by electron recombination, and equations (h) are the reactions for producing excited atomic states of mercury by collisions of metastable atoms and atoms in the imprisoned resonance states. The imprisoned resonance states of mercury are the 6^3P_1 and 6^1P_1 states which have wavelengths to the ground state of 2537$\mathring{A}$, 1850$\mathring{A}$, respectively. A resonance line is a spectral line which can be absorbed by atoms in the ground state. If the ground state atom density is large, then this radiation can become imprisoned in the cell causing an increase or extension of the lifetime of these states. This effect will only be of importance at high ground state density or in other words at high temperature in our experiment.

In order to explain the observed atomic emission spectra at various

atom densities or temperatures, the problem is to determine which mechanism holds in the different time and temperature or atom density regions. At low temperature or atom density, below 333°K the atomic photon emission and volume electron-ion recombination processes should be the dominate mechanisms for the decaying intensity. The resulting intensity of the spectral lines should be a simple exponential decay. The simple exponential has been observed for this atom density region. The natural lifetimes of the lines are around 0.01 microseconds, and the time resolution of the experimental equipment is of the order of 1 microsecond. This implies that the natural lifetimes are shorter than can be obs erved so that the initial exponential decay is controlled by volume electron recombination.

In the intermediate temperature or atom density region, above 333°K and below 433°K, the light intensity has, probably, an initial decay due to the natural lifetime of the state which can not be observed, and the rapid initial decay observed in the experiment is caused, again, by volume electron recombination. This is followed by an enhancement of the intensity caused by ionization of mercury atoms by collisions of metastable atoms, and finally a slow decay of the light intensity which is controlled by ambipolar diffusion of the electrons which are recombining with the atoms to produce excited mercury atoms.

At high temperature or atom density, above 433°K, molecular emission begins to play a role in the afterglow spectrum causing an overall drop in the intensity of the atomic spectral lines. The same processes or mechanisms still apply in this region that applied in the intermediate region, but the molecular emission is robbing the spectra of energy causing the intensity to drop.

Molecular emission is important only at high atom density for the excitation of a molecular state requires a three body atomic collision. The probability of this type of collision will only be significant at high atom densities. Molecular emission follows these mechanisms:

(i) $Hg^*_m(6^3P_o) + 2Hg \rightarrow Hg^*_{2m}(^3O_u^-) + Hg$

(j) $Hg^*_{2m}(^3O_u^-) \rightarrow Hg_2 + h\nu\,(3350\text{Å})$

(k) $Hg^*_{2m}(^3O_u^-) + 2Hg \rightarrow 4Hg + h\nu\,(4850\text{Å})$.

The molecular emission will not be discussed in detail. It will only be mentioned here. Mr. Bruce Whitcomb[12] has done work in this area and his results will be applied when necessary.

B. THE ELECTRON RATE EQUATION

The decay of the atomic radiation in the afterglow can only be explained by examining the rate equations governing electron and excited atom removal from the afterglow discharge. The rate equation for the electron density is governed by the mechanisms listed under reactions (f) and (g). The last four reactions will be ignored in the rate equation because collision of 6^1P_1 with other 6^1P_1 atoms or $6^3P_{0,1,2}$ atoms are of little importance. The 6^1P_1 state of mercury has a high probability of transition to the ground state, therefore its lifetime will be very short, and the atoms in this state will have decayed before the equipment could respond to their decay. The rate equation for the electron density is:

$$\frac{\partial e(\rho, z, t)}{\partial t} = D_e \nabla^2 e(\rho, z, t) - \alpha_1 e^- [Hg^+] + \sigma_1 [Hg(6^3P_2)]^2 \qquad (3)$$

where $e(\rho, z, t)$ is the electron density in cylindrical coordinates, $D_e \nabla^2 e(\rho, z, t)$

represents the ambipolar diffusion loss to the walls for electrons, $\alpha_1 e^- [Hg^+]$ represents the volume recombination term for Hg^+ ion and electrons, and $\sigma_1 [Hg(6^3P_2)]^2$ represents the electron production term producing electrons caused by ionizing collisions between metastable atoms.

At low atom density, electron loss is controlled by ambipolar diffusion, and electron production is controlled by ionization produced by metastable atom collisions. Thus the volume recombination loss term will be neglected. Equation (3) becomes

$$\frac{\partial e(\rho, z, t)}{\partial t} = De \nabla^2 e(\rho, z, t,) + \sigma_1 [Hg^*_m(6^3P_2)]^2 , \quad (4)$$

[I]

where the $Hg^*_m(6^3P_2)$ atom density is assumed to be of the form:

$$[Hg^*_m(6^3P_2)] = N(\rho, z, t) = A(\rho, z)\, e^{-\frac{t}{T_m}} .$$

In this equation, t is the time measured from the end of the active discharge, T_m is the lifetime of the metastable 6^3P_2 atomic state, and $A(\rho, z)$ is the metastable atom concentration of the active discharge. The solution to equation (4) is

$$e(\rho, z, t) = \sum_{i=1}^{\infty} \sum_{j=1}^{\infty} D_{ij}(\rho, z) \exp\left[-\frac{t}{\lambda_{ij}^2}\right] - \sum_{i=1}^{\infty} \sum_{j=1}^{\infty} M_{ij}(\rho, t) \exp\left[\frac{-2t}{T_m}\right] , \quad (5)$$

where $D_{ij}(\rho, z)$ is a product of zero order Bessel and cosine functions, $M_{ij}(\rho, z)$ is also a product of zero order Bessel and cosine functions, and λ_{ij}^2 is the square of the characteristic diffusion length for the electrons. If only the lowest mode of diffusion is considered, the equation reduces to the form:

[I] See Appendix I p. 42 for complete solution.

$$e(\rho, z, t) = D_{11}(\rho, z) \exp\left[-\frac{t}{\lambda_{11}^2}\right] - M_{11}(\rho, z) \exp\left[-\frac{2t}{T_m}\right] , \qquad (6)$$

where $D_{11}(\rho, z)$ is the first term of the double infinite sum, $D_{ij}(\rho, z)$; $M_{11}(\rho, z)$ is also the first term of the double infinite sum, $M_{ij}(\rho, z)$; and λ_{11} is the lowest mode characteristic diffusion length. The quantities $M_{ij}(\rho, z)$ and $M_{11}(\rho, z)$ are given by the expressions:

$$M_{ij}(\rho, z) = A_{ij}^{11}(\rho, z) \Big/ \frac{2}{T_m} - \frac{1}{\lambda_{ij}^2} ,$$

and

$$M_{11}(\rho, z) = A_{11}^{11}(\rho, z) \Big/ \frac{2}{T_m} - \frac{1}{\lambda_{11}^2} .$$

$M_{11}(\rho, z)$ is a positive constant with respect to time since $A_{11}(\rho, z)$ is positive and since the lifetime of the metastable state is smaller than the square of the characteristic diffusion length. The lowest mode of diffusion is considered the dominate mode, and other modes of diffusion are considered unobservable. The characteristic diffusion length for the lowest mode is given by the expression:

$$\frac{1}{\lambda_{11}^2} = D_e\left[\Lambda_{11}^2 + \frac{\pi^2}{H^2}\right] .$$

where Λ_{11}^2 is the lowest value of m such that $J_o(ma) = 0$, and H is the length of the cell and a is the radius of the experimental cell.

C. THE I-TH ATOMIC STATE'S RATE EQUATION

The rate equation for the decay of the i-th excited atomic state is:

$$\frac{\partial N_i(\rho, z, t)}{\partial t} = D_n \nabla^2 N_i(\rho, z, t) - a N_i(\rho, z, t) + \alpha e^-(\rho, z, t)\, Hg^+(p, z, t) \quad \text{II} \qquad (7)$$

where $N_i(\rho, z, t)$ is the atom density in the i-th excited state, $D_n \nabla^2 N_i(\rho, z, t)$ represents the diffusion loss to the walls of the cell of excited atoms, $aN_i(p, z, t)$ represents the spontaneous radiation loss from the excited state, and $\alpha e^-(\rho, z, t) \cdot Hg^+(\rho, z, t)$ is the production term caused by electron-ion recombination. It is assumed that the electron density is equal to the ion density, for the plasma is assumed neutral; thus,

$$e^-(\rho, z, t) = Hg^+(\rho, z, t).$$

In solving equation (7), the electron density term will be assumed the lowest mode electron density given by equation (6). After a suitable transformation, equation (7) is solvable. The solution is,

$$N_i(\rho, z, t) = \sum_{i=1}^{\infty} \sum_{j=1}^{\infty} F_{ij}(\rho, z) \exp\left[-t\left(\frac{1}{\delta_{ij}^2} + a\right)\right]$$

$$+ \sum_{i=1}^{\infty} \sum_{j=1}^{\infty} A_{ij}(\rho, z) \exp \frac{2t}{\lambda_{11}^2} + \sum_{i=1}^{\infty} \sum_{j=1}^{\infty} C_{ij}(\rho, z) \exp -\frac{4}{T_m}$$

$$- \sum_{i=1}^{\infty} \sum_{j=1}^{\infty} B_{ij}(\rho, z) \exp\left[-t\left(\frac{2}{T_m} + \frac{1}{\lambda_{11}^2}\right)\right],$$

where δ_{ij}^2 is the square of the characteristic diffusion length for the excited mercury atom, and $F_{ij}(\rho, z)$, $A_{ij}(\rho, z)$, $C_{ij}(\rho, z)$, and $B_{ij}(\rho, z)$ are constants times products of zero order Bessel and cosine functions. They are all constants

---

II See Appendix I. p. 54 for complete solution.

with respect to time. It will be assumed again that only the lowest mode of atom diffusion dominates.

Then equation (8) becomes

$$N_i(\rho,z,t) = F_{11}(\rho,z)\exp\left[-t\left(\frac{1}{\delta_{11}^2}+A_i\right)\right] + A_{11}(\rho,z)\exp\left(-\frac{2t}{T_m}\right) \qquad (9)$$

$$+ C_{11}(\rho,z)\exp\left(-\frac{4t}{T_m}\right)$$

$$+ B_{11}(\rho,z)\exp\left[-t\left(\frac{2}{T_m}+\frac{1}{\lambda_{11}^2}\right)\right],$$

The coefficients $F_{11}(\rho,z)$, $C_{11}(\rho,z)$, $A_{11}(\rho,z)$ and $B_{11}(\rho,z)$ are all positive first terms of the double infinite sum of coefficients of equation (8), because of the assumption that the coefficients of the electron density are all positive and that the lifetime of the metastable state is smaller than the square of the characteristic diffusion length. The other quantities have already been defined. The first exponential of the solution is that corresponding to the natural photon emission and can not be observed with our electronic equipment because of its fast decay time.

D. THE METASTABLE ATOM'S RATE EQUATION

The last rate equation to be examined is the decay of the metastable 6^3P_2 atom population. The rate equation is

$$\frac{\partial M(\rho,z,t)}{\partial t} = D_m\nabla^2 M(\rho,z,t) - \sigma_1 M^2(\rho,z,t) \qquad (10)$$

where $M(\rho,z,t)$ represents the metastable 6^3P_2 atom density, $D_m\nabla^2 M(\rho,z,t)$

[III] See Appendix I p. 67 for complete solution.

represents the loss of 6^3P_2 atoms due to diffusion to the walls, and $\sigma_1 M^2(\rho, z, t)$ the loss of metastable atoms due to collisions with similar atoms to produce electrons and Hg^+ ions. By neglecting diffusion as a loss mechanism, equation (10) becomes

$$\frac{dM(\rho, z, t)}{dt} = - \sigma_1 M^2(\rho, z, t) \tag{11}$$

Equation (11) has a solution of the form:

$$M(\rho, z, t) = \frac{A(\rho, z)}{1 + \sigma_1 A(\rho, z, t)} \simeq A(\rho, z)\, e^{- t/T_m} \tag{12}$$

where t is the time after the cut off of the active discharge, T_m is the metastable state's lifetime, and $A(\rho, z)$ is the concentration of the metastable atoms in the active discharge. In the approximation employed above $\frac{1}{T_m} = \sigma_1 A(\rho, z)$ and $M(\rho, z, 0) = A(\rho, z)$. Absorption studies have indicated that the metastable 6^3P_2 atoms decay approximately exponentially. Also, the concentration of the 6^3P_2 atoms decays to almost zero in less than 100 microseconds, and the enhancement occurs at 100 microseconds. This is the main reason that metastable atom collisions of the 6^3P_2 states were given as a possible mechanism to explain the enhancement of the light intensity.

III. EXPERIMENTAL PROCEDURE

In this experiment the experimental cell was a pyrex cylinder 300mm. long and 51mm. in diameter with pyrex windows. It had a 7mm. side arm which was used to attach the cell to a vacuum system. The cell had two tunstgen electrodes which could be used if pulsed d. c. excitation was desired. The vacuum system consisted of a rotary forepump, phosphorous pentoxide water vapor trap, and an oil diffusion pump. The cell was outgassed to a pressure of 2.2×10^{-6} mm. of Hg, the cell was heated in an oven to a temperature of 373°K, and then triply distilled mercury was distilled into the cell. The cell was then removed from the vacuum system leaving enough of the side arm attached to be used as a mercury reservoir. The cell was then encircled by an r-f tank coil tuned to 28.5Mc. Thermocouples were attached to the cell at the windows, the top, and reservoir. The cell was then placed in an oven which had pyrex end windows. The temperature was controlled by varying the current through the four heating rods of the oven.

The experimental setup is as shown in fig. 3. The signal from the r-f source, a Heathkit transmitter, was sent to the pulsed r-f power amplifier which was turned off and on 60 times a second by a screen grid switching signal. The resultant signal from the power amplifier was then impedance matched to the mercury cell where the signal produced an intense r-f discharge. The radiation from the cell was focused into a Bausch & Lomb 500mm. quartz grating monochromator and detected with an EMI 6256Q quartz windowed photomultiplier which was powered by a Fluke 412B power supply. The current from

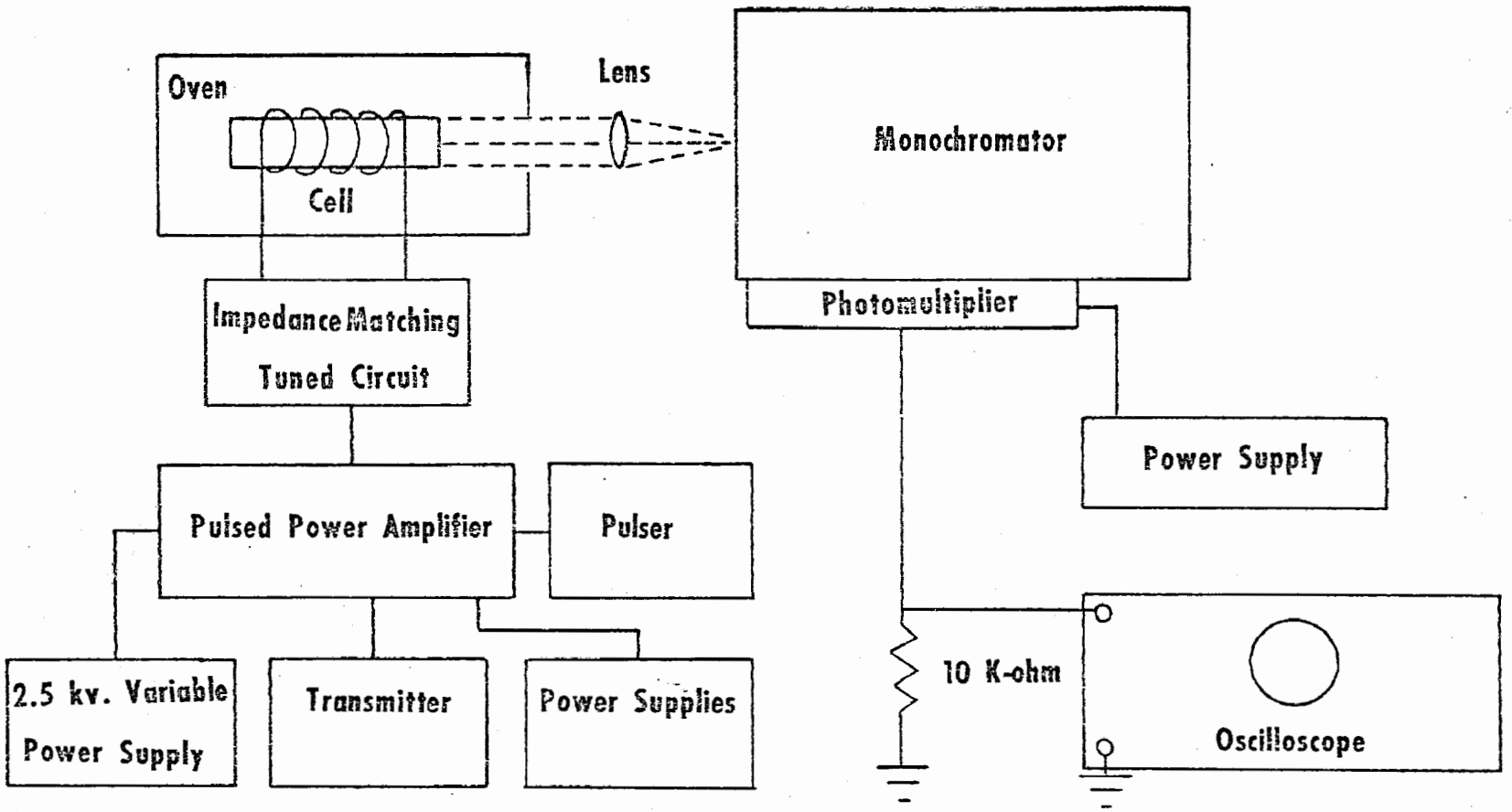

Figure 3. Block diagram of the apparatus used in the experiment.

the photomultiplier was sent through a 10Kohm resistor and the voltage across the resistor was displayed on a 531A Tektronix oscilloscope. In order to synchronize the oscilloscope, the horizontal sweep was triggered externally when the power amplifier was pulsed off. This trigger was supplied by the 60 cycle switching pulser for the power amplifier.

The monochromator was used to separate the different wavelengths of mercury light. The temperature of the oven and cell was varied by controlling the current in the heating rods. The r-f power input to the discharge was varied by controlling the plate voltage supply to the amplifier. Polaroid pictures were then taken of the various spectral lines displayed. The spectral lines examined were of wavelengths 5771, 5462, 4360, 4079, 4047, 3907, 3657/56, 3342, and 3327/32$\mathring{A}$. These lines were examined at cell temperatures of 333^{o}K, 353^{o}K, 373^{o}K, 398^{o}K, 423^{o}K, 433^{o}K, 443^{o}K, 453^{o}K, 463^{o}K, 473^{o}K, and 498^{o}K. Finally, each line at each temperature was examined at four r-f power levels of 200, 400, 500, and 600 watts.

IV. RESULTS AND DISCUSSION

A. THE COMPARISON BETWEEN THEORY AND EXPERIMENT OF THE AFTERGLOW SPECTRA

The comparison of theory and experimental data is shown in figure 4 and 5. The solid line is the theoretical curve, and the circles indicate the direction of the experimental curve for the light intensity versus time. The comparison of theory and experiment is for the representative lines 5771, 5462, 4362, 4079, 4947, 3907, 3651/56, and 3127/32Å of mercury at 398°K. At 398°K, the enhancement effect has become pronounced and molecular emission has not entered into the afterglow spectrum because of the low mercury atom density. The theory predicts that the light intensity of the atomic lines of mercury follows four exponential decaying terms, but because the experimental equipment had a rise time of approximately 1 microsecond and the expected decay time of natural radiation is of the order of.01 microseconds only three exponentials were observed. The decay constant $\frac{1}{\delta_{11}^2} + a$ was not observed. In Table I., the coefficients A_{11}, B_{11}, and C_{11} are tabulated for the lines mentioned above. The decay constants $\frac{2}{\lambda_{11}^2}$, $\frac{1}{\lambda_{11}^2} + \frac{2}{T_m}$, and $4/T_m$ are also tabulated. From these decay constants and the dimensions of the cell, an average value of the electron ambipolar diffusion constant, D_e, and the lifetime of the metastable 6^3P_2 state of mercury, T_m, can be evaluated. The average value of D_e is 991 cm^2/sec. The average value of T_m is 47 microseconds.

B. THE ENHANCEMENT OF THE ATOMIC LINES

Figures 6, 7, and 8 show the intensity behavior versus time and r-f

power input to the mercury discharge at temperatures of 33, 373, 423, and 473°K. On each figure, there are four r-f power levels corresponding to 600, 500, 400, and 200 watts. The largest power input is the first curve in the figure and the three other power levels are displaced approximately 100 microseconds from each other. All atomic lines of mercury exhibit the enhancement effect. The 4079Å line, which is an intercombination line and weak in intensity, originates from the 7^1S_0 state, and did exhibit an enhancement at 150°K which disagrees with the experiment of Stepp and Anderson.[7] The 4079Å line decays in a simple exponential fashion for all temperature and power levels below 423°K, and is assumed to be controlled by volume electron-ion recombination in this region. The lines 3651/56 and 3127/32Å which originate from the 6^3D_3 and 6^3D_1 states exhibit enhancement which is greater than the intensity of the line in the active discharge. This implies a high population of these states in the afterglow. The lines 5462, 4360, and 4047Å which originate from the 7^3S_1 state are not intercombination lines and exhibit an enhancement, but the intensity is never greater than the intensity of the line in the active discharge. The 5771Å line is an intercombination line which shows an enhancement, but is never greater than the intensity of the active discharge. This data is tabulated in Table II.

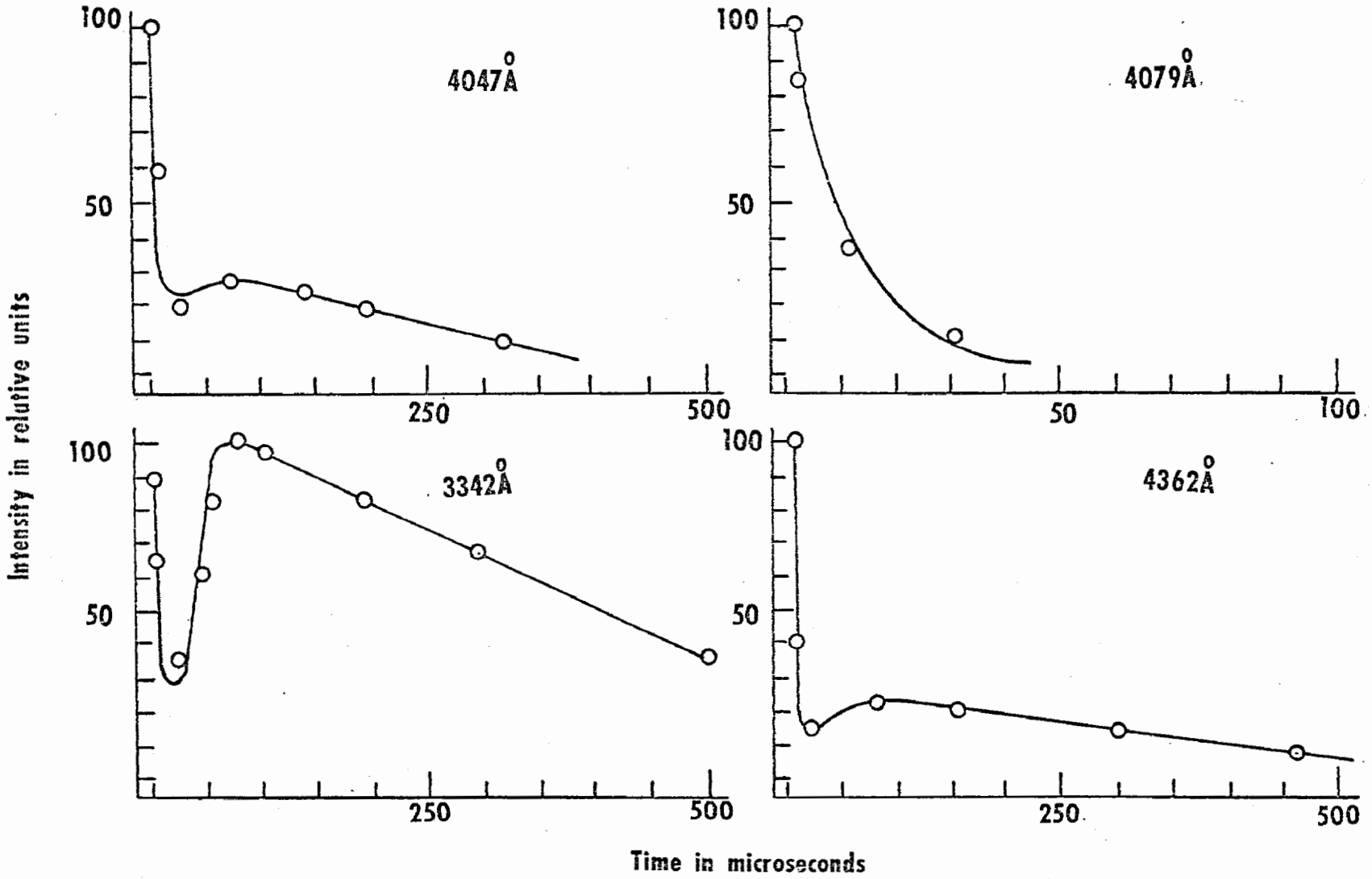

Figure 4. Comparison of theory and results for selected lines of mercury at 398° K.

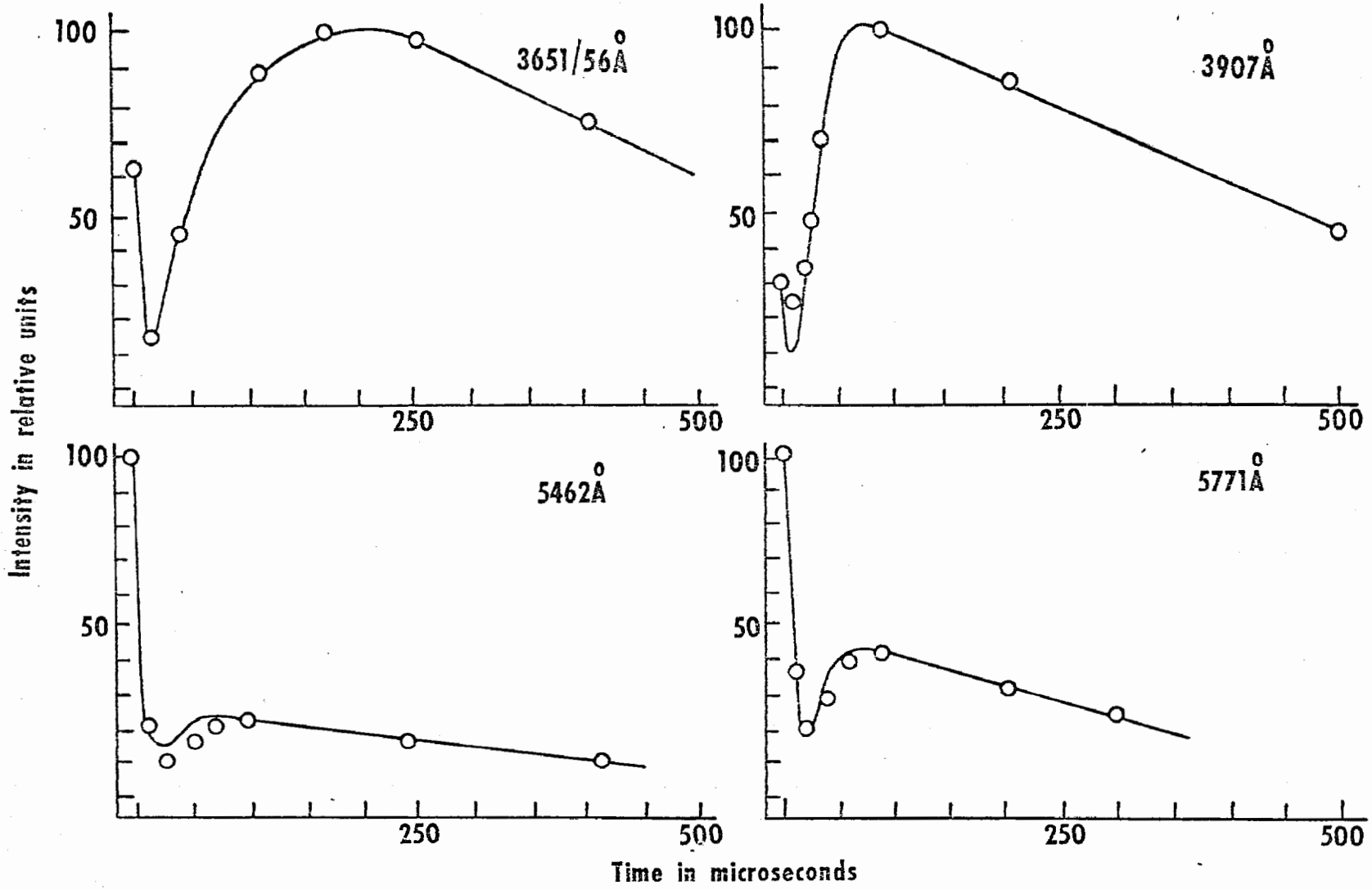

Figure 5. Comparison of theory and results for selected lines of mercury at 398°K.

TABLE I

Wavelength of the Atomic Line	A_{11}^{*}	B_{11}^{*}	C_{11}^{*}	$\frac{4}{T_m}$ X10^{+6}	$\frac{2}{\lambda_{11}^2}$ X10^{+6}	$\frac{1}{\lambda_{11}^2} + \frac{2}{T_m}$ X10^{+6}	D_e cm^2/sec	T_m X10^{-6} sec.
4047Å	28	75	147	.090	.0016	.055	800.0	44.4
4079Å	-	-	122	.090	-	-	-	44.4
5462Å	27	325	398	.078	.0015	.066	750.8	51.2
5771Å	51	330	379	.085	.0025	.062	1250.6	47.1
3340Å	125	333	296	.080	.0021	.042	1250.1	50.0
3907Å	122	450	358	.090	.0018	.052	900.0	44.4
3651/56Å	195	270	358	.057	.0021	.012	1200.3	71.4

*AVERAGE VALUE OF D_e = 991 cm^2/sec. AVERAGE VALUE OF T_m = 47 microsec.

*Relative Units of Intensity

** The 3651/56Å atomic line was omitted when averages were calculated.

TABLE I - LIST OF COEFFICIENTS AND DECAY CONSTANTS

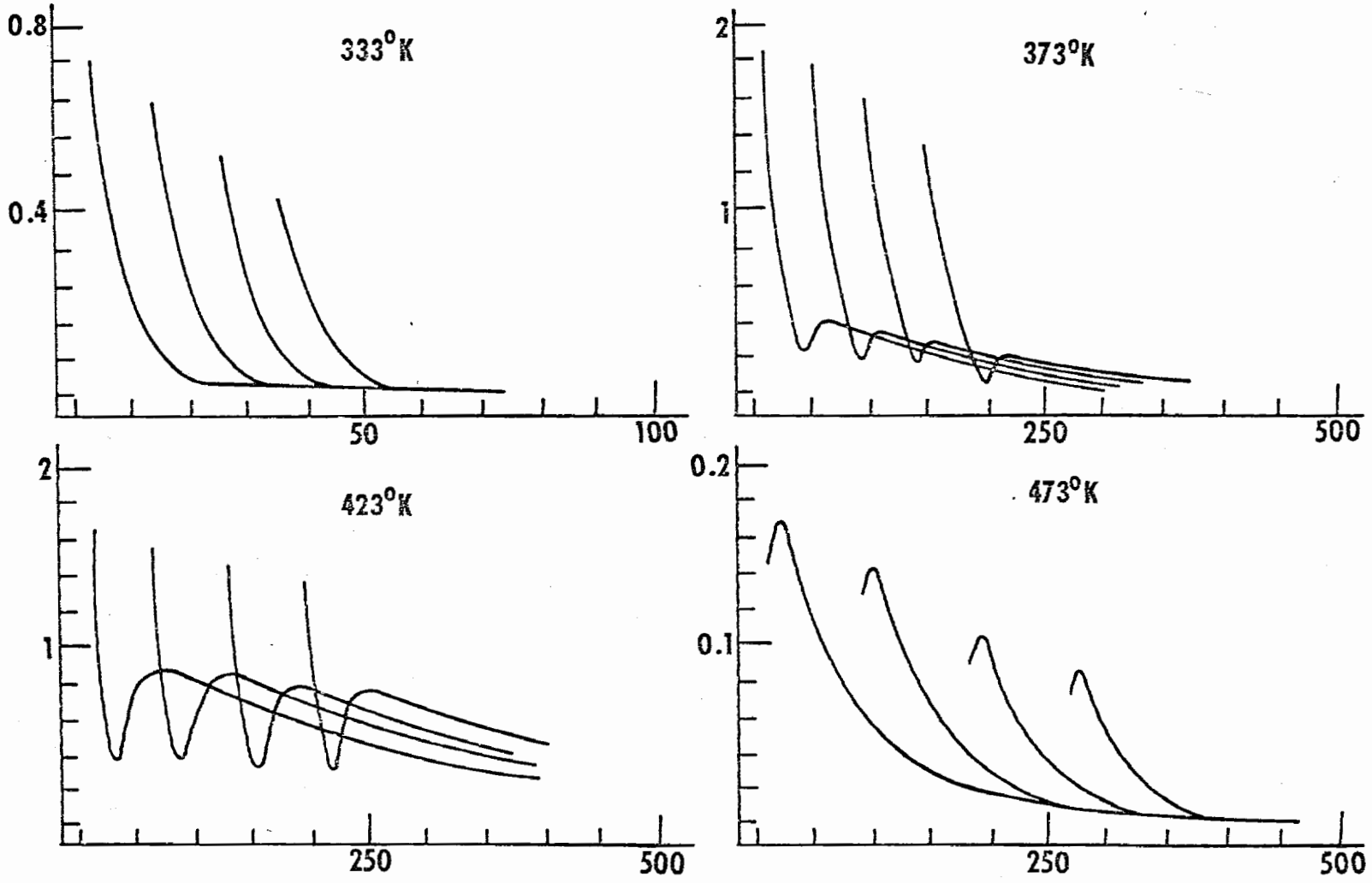

Figure 6. Decay of light intensity versus time for the 5771Å line.

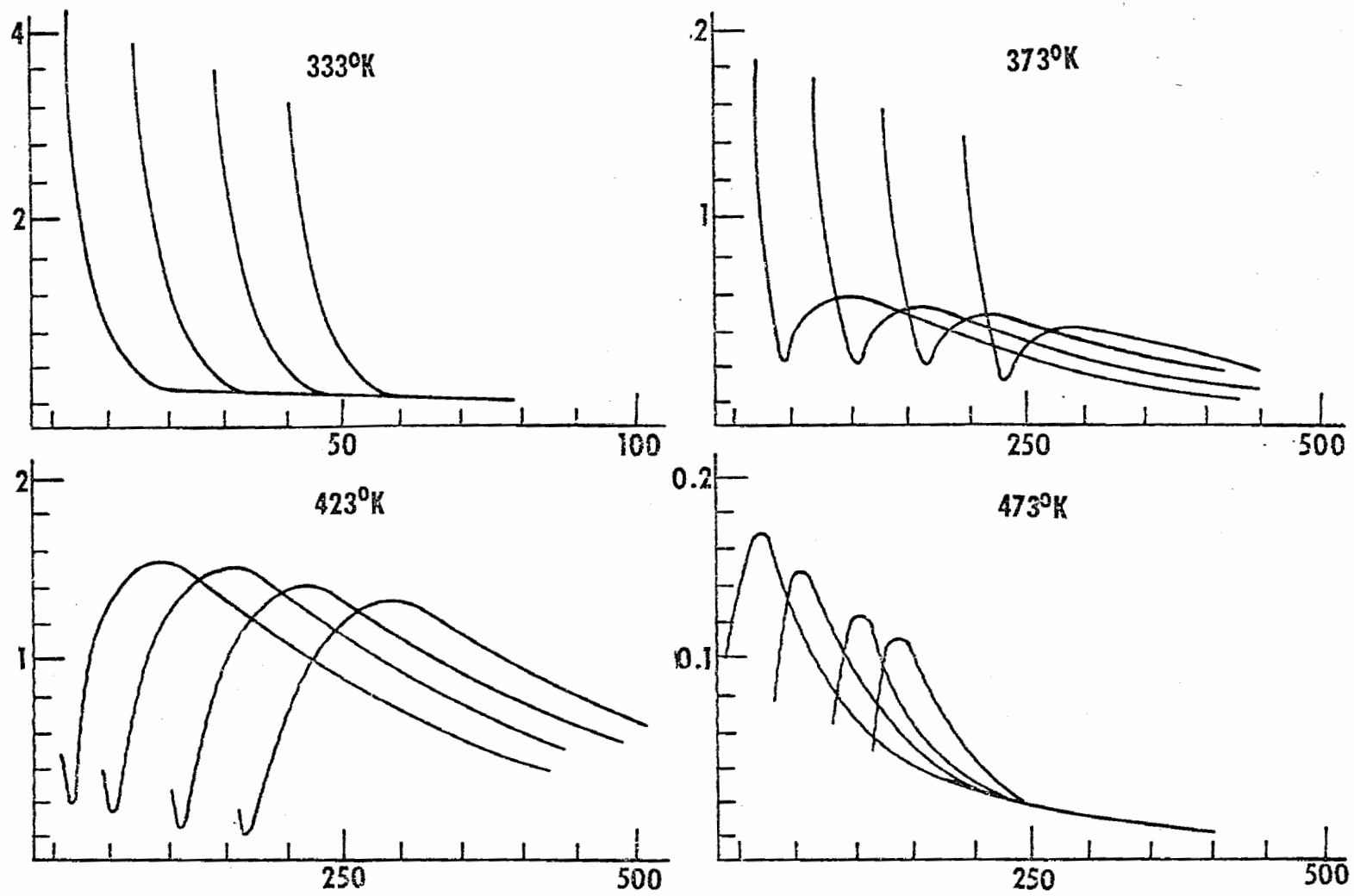

Fiure 7. Decay of light intensity versus time for the 3651/56Å line.

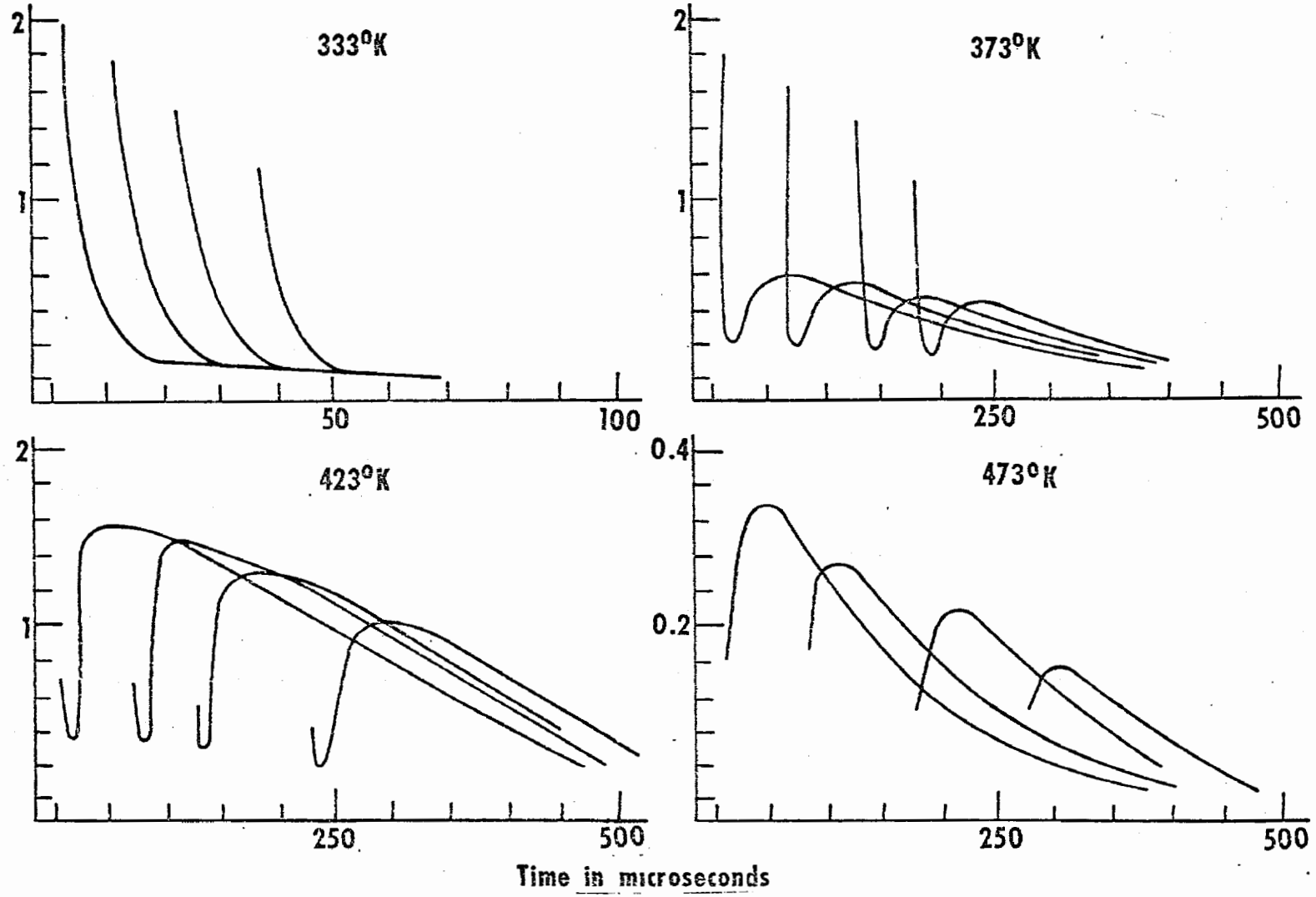

Figure 8. Decay of light intensity versus time for the 3127/32Å line.

TABLE II - Intensity of the lines at the positions of minimum of the initial drop (columns A) and the maximum of the enhancement (columnsB) immediately after shut off of the discharge as a percentage of the intensity just before shut off. A blank space indicates that the line did not drop initially in intensity and an asterisk indicates that the line decayed in a smooth exponential fashion.

Wavelength, transition, and energy	Temperature 333°K							
of originating state in selection volts	P_1 = 600 watts		P_2 = 500 watts		P_3 = 400 watts		P_4 = 200 watts	
	A%	B%	A%	B%	A%	B%	A%	B%

All atomic spectra lines of mercury decayed in a smooth exponential fashion for temperatures below 333°K.

- TABLE II (CONTINUED) -

Wavelength, transition, and energy of originating state in electron volts			Temperature 353°K P_1 = 600 watts A%	B%	P_2 = 500 watts A%	B%	P_3 = 400 watts A%	B%	P_4 = 200 watts A%	B%
3651/56Å	$6^3D_{3,2}$-6^3P_2	(8.85)	5.5	20.1	5.8	9.6	4.5	18.2	6.2	17
5771	6^3D_2-6^1P_1	(8.84)	5.5	9.0	5.8	9.6	4.6	6.7	6.0	8.0
4079	7^1S_0-6^3P_2	(7.92)	*	*	*	*	*	*	*	*
4360	7^3S_1-6^3P_1	(7.73)	*	*	*	*	*	*	*	*
5462	7^3S_1-6^3P_2	(7.73)	*	*	*	*	*	*	*	*
4047	7^3S_1-6^3P_0	(7.73)	*	*	*	*	*	*	*	*
3342	8^3S_1-6^3P_2	(9.17)	8.0	20.0	7.0	19.0	7.8	18.1	6.0	15.4
3907	8^1D_2-6^1P_1	(9.87)	50.0	97.1	No Data Taken					
3127/32	$6^3D_{2,1}$-6^3P_1	(8.84)	6.3	18.0	5.4	17.2	4.5	14.0	5.2	15.6

- TABLE II (CONTINUED) -

Wavelength, transition, and energy of originating state in electron volts			Temperature 373°K P_1 = 600 watts A%	B%	P_2 = 500 watts A%	B%	P_3 = 400 watts A%	B%	P_4 = 200 watts A%	B%
3651/56Å	$6^3D_{3,2}-6^3P_2$	(8.85)	10.1	38.0	11.2	36.0	13.0	39.5	12.3	36.0
5771	$6^3D_2-6^1P_1$	(8.84)	5.8	11.1	4.0	11.7	5.0	12.5	5.6	11.5
4079	$7^1S_0-6^3P_2$	(7.92)	*	*	*	*	*	*	*	*
4360	$7^3S_1-6^3P_1$	(7.73)	9.1	15.0	7.5	14.5	5.0	11.5	4.0	6.5
5462	$7^3S_1-6^3P_2$	(7.73)	11.4	22.0	11.6	21.4	10.1	16.5	7.8	13.4
4047	$7^3S_1-6^3P_0$	(7.73)	*	*	*	*	*	*	*	*
3342	$8^3S_1-6^3P_2$	(9.17)	12.6	32.0	9.0	30.9	8.0	29.5	8.5	28.2
3907	$8^1D_2-6^1P_1$	(9.87)	46.1	166.3	35.6	160.3	50.4	200.1	30.1	150.2
3127/32	$6^3D_{2,1}-6^3P_1$	(8.84)	8.7	29.3	7.2	28.4	7.5	26.1	5.4	24.2

- TABLE II (CONTINUED) -

Wavelength, transition, and energy of originating state in electron volts			Temperature 398°K P_1 = 600 watts A%	B%	P_2 = 500 watts A%	B%	P_3 = 400 watts A%	B%	P_4 = 200 watts A%	B%
3651/56Å	$6^3D_{3,2}$-6^3P_2	(8.85)	26.2	166.5	28.1	169.1	27.3	165.2	22.3	170.5
5771	6^3D_2-6^1P_1	(8.84)	20.4	41.6	20.9	43.4	17.9	38.3	16.8	45.8
4079	7^1S_0-6^3P_2	(7.92)	*	*	*	*	*	*	*	*
4360	7^3S_1-6^3P_1	(7.73)	12.8	22.2	11.4	20.3	13.2	20.0	9.7	20.3
5462	7^3S_1-6^3P_2	(7.73)	10.0	25.5	5.1	24.3	6.8	20.4	5.6	19.2
4047	7^3S_1-6^3P_0	(7.73)	*	*	*	*	*	*	*	*
3342	8^3S_1-6^3P_2	(9.17)	39.2	115.2	36.2	111.7	32.5	107.4	30.1	113.5
3907	8^1D_2-6^1P_1	(9.87)	57.2	222.1	57.2	230.0	51.8	231.1	46.8	228.9
3127/32	$6^3D_{2,1}$-6^3P_1	(8.84)	No Data Taken							

- TABLE II (CONTINUED) -

Wavelength, transition, and energy of originating state in electron volts			Temperature 423°K P_1 = 600 watts A%	B%	P_2 = 500 watts A%	B%	P_3 = 400 watts A%	B%	P_4 = 200 watts A%	B%
3651/56Å	$6^3D_{3,2}-6^3P_2$	(8.85)	58.1	294.5	50.0	290.0	44.5	292.4	50.0	285.5
5771	$6^3D_2-6^1P_1$	(8.84)	37.7	70.1	34.4	68.1	31.1	65.5	30.3	65.0
4079	$7^1S_0-6^3P_2$	(7.92)	Slight Enhancement at all Powers							
4360	$7^3S_1-6^3P_1$	(7.73)	16.6	26.5	17/7	24.4	15.4	27.3	16.9	26.2
5462	$7^3S_1-6^3P_2$	(7.73)	22.5	45.1	22.2	44.4	20.1	40.2	20.0	45.2
4047	$7^3S_1-6^3P_0$	(7.73)	16.2	20.0	14.2	17.7	13.5	16.7	11.1	15.9
3342	$8^3S_1-6^3P_2$	(9.17)	33.3	156.3	36.4	190.3	35.8	180.1	25.5	180.1
3907	$8^1D_2-6^1P_1$	(9.87)		410.0		382.2		400.0		420.1
3127/32	$6^3D_{2,1}-6^3P_1$	(8.84)	46.6	154.8	45.5	151.5	43.6	160.0	40.3	151.8

- TABLE II (CONTINUED) -

Wavelength, transition, and energy of originating state in electron volts			Temperature 433°K P_1 = 600 watts A%	B%	P_2 = 500 watts A%	B%	P_3 = 400 watts A%	B%	P_4 = 200 watts A%	B%
3651/56Å	$6^3D_{3,2}-6^3P_2$	(8.85)	69.2	211.4	58.9	195.5	68.1	218.3	60.3	180.0
5771	$6^3D_2-6^1P_1$	(8.84)	65.5	70.7	61.3	100.0	62.0	94.0		
4079	$7^1S_0-6^3P_2$	(7.92)	*	*	*	*	*	*	*	*
4360	$7^3S_1-6^3P_1$	(7.73)	35.5	44.4	34.0	42.2	29.9	39.1	83.3	96.0
5462	$7^3S_1-6^3P_2$	(7.73)	40.0	68.8	39.5	64.4	28.3	60.2		162.3
4047	$7^3S_1-6^3P_0$	(7.73)	*	*	*	*	*	*	*	*
3342	$8^3S_1-6^3P_2$	(9.17)	80.7	216.3	74.5	208.8	80.0	246.5	83.3	191.1
3907	$8^1D_2-6^1P_1$	(9.87)		344.4		313.3		333.3		375.0
3127/32	$6^3D_{2,1}-6^3P_1$	(8.84)	62.1	172.2	61.0	171.5	55.5	165.8	50.0	116.6

- TABLE II (CONTINUED) -

Wavelength, transition, and energy of originating state in electron volts			Temperature 443°K P_1 = 600 watts A%	B%	P_2 = 500 watts A%	B%	P_3 = 400 watts A%	B%	P_4 = 200 watts A%	B%
3651/56Å	$6^3D_{3,2}-6^3P_2$	(8.85)	86.6	196.5	77.4	152.3		173.3		171.3
5771	$6^3D_2-6^1P_1$	(8.84)	77.4	103.0	70.0	100.0		130.1		140.4
4079	$7^1S_0-6^3P_2$	(7.92)	*	*	*	*	*	*	*	*
4360	$7^3S_1-6^3P_1$	(7.73)	45.3	50.0	40.8	41.1	*	*	*	*
5462	$7^3S_1-6^3P_2$	(7.73)	50.5	75.3	41.6	66.6		137.7		136.3
4047	$7^3S_1-6^3P_0$	(7.73)	*	*	*	*	*	*	*	*
3342	$8^3S_1-6^3P_2$	(9.17)		196.5		187.6	*	*	*	*
3907	$8^1D_2-6^1P_1$	(9.87)		222.1		256.4	*	*	*	*
3127/32	$6^3D_{2,1}-6^3P_1$	(8.84)		192.7		158.0		120.7		115.3

- TABLE II (CONTINUED) -

Wavelength, transition, and energy of originating state in electron volts			Temperature 453°K P_1 = 600 watts A%	B%	P_2 = 500 watts A%	B%	P_3 = 400 watts A%	B%	P_4 = 200 watts A%	B%
3651/56Å	$6^3D_{3,2}-6^3P_2$	(8.85)		250.0		259.0		220.5		225.5
5771	$6^3D_2-6^1P_1$	(8.84)	80.1	90.9		126.5		124.7		130.7
4079	$7^1S_0-6^3P_2$	(7.92)	*	*	*	*	*	*	*	*
4360	$7^3S_1-6^3P_1$	(7.73)	*	*	*	*	*	*	*	*
5462	$7^3S_1-6^3P_2$	(7.73)	50.3	70.4	50.1	60.6	74.7	85.5	81.3	94.8
4047	$7^3S_1-6^3P_0$	(7.73)	*	*	*	*	*	*	*	*
3342	$8^3S_1-6^3P_2$	(9.17)	No Data Taken							
3907	$8^1D_2-6^1P_1$	(9.87)	No Data Taken							
3127/32	$6^3D_{2,1}-6^3P_1$	(8.84)	No Data Taken							

- TABLE II (CONTINUED) -

Wavelength, transition, and energy of originating state in electron volts			Temperature 463°K P_1 = 600 watts A%	B%	P_2 = 500 watts A%	B%	P_3 = 400 watts A%	B%	P_4 = 200 watts A%	B%
3651/56Å	$6^3D_{3,2}$-6^3P_2	(8.85)		295.1		303.3		295.4		250.7
5771	6^3D_2-6^1P_1	(8.84)		155.3		125.6		134.2		136.6
4079	7^1S_0-6^3P_2	(7.92)	*	*	*	*	*	*	*	*
4360	7^3S_1-6^3P_1	(7.73)	*	*	*	*	*	*	*	*
5462	7^3S_1-6^3P_2	(7.73)	87.7	97.1	77.0	88.8	77.1	100.0	80.0	92.5
4047	7^3S_1-6^3P_0	(7.73)	*	*	*	*	*	*	*	*
3342	8^3S_1-6^3P_2	(9.17)	*	*	*	*	*	*	*	*
3907	8^1D_2-6^1P_1	(9.87)		125.5		125.9	*	*	*	*
3127/32	$6^3D_{2,1}$-6^3P_1	(8.84)		250.4		244.3		212.4		200.0

- TABLE II (CONTINUED) -

Wavelength, transition, and energy of originating state in electron volts			Temperature 473°K P_1 = 600 watts A%	B%	P_2 = 500 watts A%	B%	P_3 = 400 watts A%	B%	P_4 = 200 watts A%	B%
3651/56Å	$6^3D_{3,2}-6^3P_2$	(8.85)		20.1		235.2		240.0		204.5
5771	$6^3D_2-6^1P_1$	(8.84)		168.9		153.5		123.3		150.0
4079	$7^1S_0-6^3P_2$	(7.92)	*	*	*	*		*	*	*
4360	$7^3S_1-6^3P_1$	(7.73)	*	*	*	*		*	*	*
5462	$7^3S_1-6^3P_1$	(7.73)		114.4		122.9		114.5		120.7
4047	$7^3S_1-6^3P_0$	(7.73)	*	*		*		*		*
3342	$8^3S_1-6^3P_2$	(9.17)		130.2		125.4		123.1		116.2
3907	$8^1D_2-6^1P_1$	(9.87)				No Data Taken				
3127/32	$6^3D_{2,1}-6^3P_1$	(8.84)		173.6		180.0		175.3		175.8

- TABLE II (CONTINUED) -

Wavelength, transition, and energy of originating state in electron volts			Temperature 498°K P_1 = 600 watts A%	B%	P_2 = 500 watts A%	B%	P_3 = 400 watts A%	B%	P_4 = 200 watts A%	B%
3651/56Å	$6^3D_{3,2}$-6^3P_2	(8.85)		290.1		312.3		285.4		233.3
5771	6^3D_2-6^1P_1	(8.84)		168.3		160.6		184.7		166.0
4079	7^1S_0-6^3P_2	(7.92)	*	*	*	*	*	*	*	*
4360	7^3S_1-6^3P_1	(7.73)	*	*	*	*	*	*	*	*
5462	7^3S_1-6^3P_2	(7.73)	76.1	87.6	76.0	105.0	76.5	82.4	76.1	76.3
4047	7^3S_1-6^3P_0	(7.73)	*	*	*	*	*	*	*	*
3342	8^3S_1-6^3P_2	(9.17)	*	*	*	*	*	*	*	*
3907	8^1D_2-6^3P_1	(9.87)			No Data Taken					
3127/32	$6^3D_{2,1}$-6^3P_1	(8.84)		245.5		225.4		218.6		212.3

IV. CONCLUSION

Several conclusions can be reached from this experiment. It was assumed in the theory for the process occurring in the discharge that at low atom densities, two mechanisms were controlling the electron density. Ambipolar diffusion of the electrons from an elemental volume in the discharge was the main mechanism for the loss of electrons. Electrons were assumed to be produced by metastable 6^3P_2 atom collisions. From these assumptions, an expression for the electron density can be obtained. On making the assumption that the plasma is neutral and that the electron density is equal to the mercury ion density, one, the enhancement effect observed in an r-f excited mercury discharge for the light intensity of the atomic lines can be predicted. Two, the cause of the enhancement can be concluded to be the metastable atom collisions which produce ionization of mercury atoms. The subsequent electron-ion recombination produces excited mercury atoms which radiate energy. Three, the observed decay of the atomic lines can be predicted to be three exponential functions. The rapid initial decay is produced by volume electron recombination, the enhancement is produced by metastable 6^3P_2 atom collisions, and the final long decay is controlled by volume electron recombination of electrons with mercury ions which is controlled by ambipolar diffusion at low temperatures. Four, in the experiment, the r-f power to the discharge was varied, and the modes of decay were observed not to be a function of r-f power to the discharge. As should be expected, only the light intensity of the atomic lines was observed to vary with power. Five, from the comparison of theory and results, certain constants could be calculated. The average value of the

ambipolar diffusion coefficient was calculated to have the value $D_e = 991$ $cm^2/sec.$; the metastable 6^3P_2 state's lifetime was calculated to have the value $T_m = 47$ microseconds.

BIBLIOGRAPHY

1. McDaniel, E.W., Collisions Phenomena in Ionized Gases, New York, John Wily & Son Inc., p. 775 (1964).

2. Sayers, J., "Ionic Recombination In Air", Proc. Roy, Soc., A-169, p. 83 (1938).

3. Stepp, E. and Anderson, R., "Decay of Intensity of Certain Hg Lines in an Hg-Ar Discharge", J. Opt. Soc. Am., 53, pp. 1139-46 (1963).

4. Niles, N.E. and Robertson, W.W., "Atomic Emission of the Helium Afterglow", J. Chem. Phys., 40, pp. 3568-71 (1964).

5. Mosbury, E.R., "Recombination of He and He in the Afterglow of a Helium Discharge", Phys. Rev., 152, pp. 152-76 (1966).

6. Biondi, M.A., "Processes Involving Ions and Metastable Atoms in Mercury Afterglow", Phys. Rev., 90, pp. 730-37 (1953).

7. Stepp, E. and Anderson, R., Spectragraphic Study of the Afterglow of Mercury", J. Opt. Soc. Am., 55, pp. 31-33 (1965).

8. McCoubrey, A.O., "The Band Fluorescence of Mercury Vapor", Phys. Rev., 93, pp. 1249-60 (1954).

9. Kunkel, W.H., "Analysis of Ionic Recombination Including Ion Production During Measurements", Phys. Rev., 84, pp. 218-21 (1951).

10. Kenty, C., "Production of 2537Å Radiation and the Role of Metastable Atoms in an Ar-Hg Discharge", J. Appl. Phys., 21, pp. 1309-18 (1950).

11. Yokoyama, M., "Absorption Studies of Metastable Mercury Atoms in an Ar-Hg Discharge Afterglow", Sci of Light, 8, pp. 59-66 (1959).

12. Whitcomb, B.W., "A Study of the Molecular Emission and the Lifetime of the Metastable States in the Afterglow Spectrum of a Mercury Discharge", Master's Thesis, The University of Missouri at Rolla (1967).

VITA

The author was born January 20, 1944 in Wichita, Kansas. His parents are Mr. and Mrs. Anthony J. Aubrecht who now reside in Kansas City, Missouri. He obtained the degree of Bachelor of Science from the University of Missouri at Rolla in August of 1965. He started graduate study in September of 1965 at the University of Missouri at Rolla. He has held a teaching assistantship during the past two years in the Physics Department.

APPENDIX I

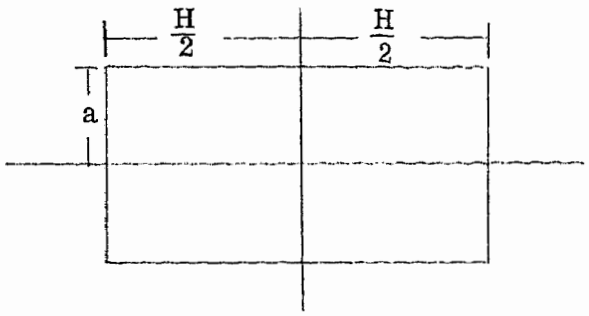

The above diagram is schematic of the experimental cell. The rate equation for the removal of electrons from the afterglow of mercury is:

$$\frac{\partial e(\rho,z,t)}{\partial t} = D_e \nabla^2 e(\rho,z,t) + \sigma_1 [H_g(6^3P_2)]^2, \qquad (1)$$

where $e(\rho,z,t)$ is the electron density, $D_e \nabla^2 e(\rho,z,t)$ represents the ambipolar diffusion loss to the walls for electrons, and $\sigma_1 [H_g(6^3P_2)]^2$ represents the production term for electrons associated with ionizing collisions between 6^3P_2 metastable atoms of mercury. The boundary conditions are:

$$e(a,z,t) = e(\rho, \pm \frac{H}{2}, t) = 0 \text{ and } e(\rho,z,o) = F(\rho,z). \qquad (2)$$

In the boundary conditions, it is assumed that there are no electrons at the walls of the cell, and that the electron concentration is $F(\rho,z)$ at the end of the active discharge. The solution of equation (1) is of the form:

$$e(\rho,z,t) = e_1(\rho,z,t) + e_2(\rho,z,t), \qquad (3)$$

and it is governed by the boundary conditions:

$$e(a,z,t) = e(\rho, \pm, \frac{H}{2}) = 0 \text{ and } e(\rho,z,t) = f_1(\rho,z) + f_2(\rho,z) = F(\rho,z). \qquad (4)$$

where $e_1(\rho,z,t)$ is the general solution, and $e_2(\rho,z,t)$ is any particular solution of equation (1). $e_1(\rho,z,t)$ is the solution of the partial differential equation:

$$\frac{\partial e_1(\rho,z,t)}{\partial t} = D_e \nabla^2 e_1(\rho,z,t), \tag{5}$$

under the boundary conditions:

$$e_1(a,z,t) = e_1(\rho,\pm\frac{H}{2},t) = 0 \text{ and } e_1(\rho,z,o) = f_1(\rho,z) . \tag{6}$$

$e_2(\rho,z,t)$ is any solution of the partial differential equation:

$$\frac{\partial e_2(\rho,z,t)}{\partial t} = D_e \nabla^2 e_2(\rho,z,t) + \sigma_1 N(\rho,z,t), \tag{7}$$

where it is assumed that $N(\rho,z,t) = [H_g(6^3P_2)]^2 = A^2(\rho,z,t)e^{\frac{-2t}{T_m}}$ is the production term for electrons due to collisions of the 6^3P_2 metastable state of mercury. The boundary conditions are:

$$e_2(a,z,t) = e_2(\rho,\pm\frac{H}{2},t) = 0 \quad e_2(\rho,z,o) = f_2(\rho,z). \tag{8}$$

In order to solve equation (5), the solution is assumed to be of the form:

$$e_1(\rho,z,t) = X(\rho,z)\,\Phi\,(t). \tag{9}$$

When equation (9) is substituted into equation (5) it becomes:

$$\begin{aligned} \frac{X d\Phi}{dt} &= \Phi D_e \nabla^2 X \\ \frac{1}{\Phi}\frac{d\Phi}{dt} &= \frac{D_e \nabla^2 X}{X} = -\frac{1}{\lambda^2} . \end{aligned} \tag{10}$$

After separation of variables, two differential equations must be solved to find the solution for $e_1(\rho,z,t)$. These differential euqations are:

$$\frac{1}{\Phi}\frac{d}{dt} = -\frac{1}{\lambda^2}, \tag{11}$$

and

$$\nabla^2 X + \frac{X}{D_e \lambda^2} = 0. \tag{12}$$

The solution of equation (11) can be found by straightforward integration which yields:

$$\Phi(t) = Ce^{-\frac{t}{\lambda^2}} \tag{13}$$

The coordinate equation (12) may be solved by assuming a solution of the form:

$$X(\rho, z) = R(P)\,\Theta(z), \tag{14}$$

and upon substituting equation (14) into equation (12), it becomes:

$$\frac{1}{R}\left(\frac{d^2R}{d\rho^2} + \frac{1}{R}\frac{dR}{d\rho}\right) + \frac{1}{D_e\lambda^2} = -\frac{1}{\Theta}\frac{d^2\Theta}{dz^2} = k^2 \tag{15}$$

After this separation of variables, equation (15) becomes two differential equations:

$$\frac{1}{\Theta}\frac{d^2\Theta}{dz^2} - k^2 = 0, \tag{16}$$

and

$$\frac{d^2R}{d\rho^2} + \frac{1}{\rho}\frac{dR}{d\rho} + \left(\frac{1}{D_e\lambda^2} - k^2\right)R = 0. \tag{17}$$

Equation (17) will be solved first and Λ^2 will be substituted for the term $\frac{1}{D_e\lambda^2} - k^2$. Equation (17) becomes:

$$\frac{d^2R}{d\rho^2} + \frac{1}{\rho}\frac{dR}{d\rho} + \Lambda^2 R = 0, \tag{18}$$

which is Bessel's differential equation of the form:

$$\frac{d^2R}{d\rho^2} + \frac{1}{\rho}\frac{dR}{d\rho} + (m^2 - n^2)R = 0,$$

and has possible solutions of the form:

$$R(\rho) = A_{mn}J_n(m\rho) + B_{mn}Y_n(m\rho).$$

From the behavior of the function $Y_n(m\rho)$, that $Y_n(m\rho) \rightarrow \infty$ as $\rho \rightarrow 0$, B_{mn} must be zero to have realistic solutions. In our equation, m and n are given by the relationships:

$$n = 0 \quad \text{and} \quad m^2 = \Lambda^2 = \frac{1}{D_e \lambda^2} - k^2 \tag{19}$$

The most general solution to equation (17) is a sum of Bessel's functions:

$$R(\rho) = \sum_{m=1}^{\infty} A_m J_o(\Lambda\rho), \tag{20}$$

Equation (16), $\frac{1}{\Theta} \frac{d^2\Theta}{dz^2} - K^2 = 0$, will now be solved. A possible solution is:

$$\Theta(z) = E e^{ikz} + G e^{-ikz} \tag{21}$$

Equation (21) must obey the boundary conditions:

$\Theta(\frac{H}{2}) = \Theta(-\frac{H}{2}) = 0$; then:

$$\Theta(\frac{H}{2}) = 0 = E e^{\frac{ikH}{2}} + G e^{\frac{-ikH}{2}}$$

and

$$\Theta(-\frac{H}{2}) = 0 = E e^{\frac{-ikH}{2}} + G e^{\frac{ikH}{2}},$$

Upon adding the equations above, the result is:

$$\Theta(\frac{H}{2}) + \Theta(\frac{H}{2}) = 0 = E(e^{\frac{ikH}{2}} + e^{\frac{-ikH}{2}}) + G(e^{\frac{ikH}{2}} + e^{\frac{-ikH}{2}}),$$

but $\cos\frac{kH}{2} = \frac{e^{\frac{ikH}{2}} + e^{\frac{-ikH}{2}}}{2}$, so $0 = (E+G)\, 2\cos\frac{kH}{2}$

This equation will only be zero if:

$$\frac{kH}{2} = (2j - 1)\frac{\pi}{2},$$

$$k_j = (2j - 1)\frac{\pi}{H} \quad \text{where } j = 1, 2, 3 \ldots\ldots \tag{22}$$

Upon substituting equation (22) into equation (21), it becomes:

$$\Theta(z) + Ee^{i(2j-1)\frac{\pi z}{H}} + Ge^{i(2j-1)\frac{\pi z}{H}}, \tag{23}$$

where $j = 1,2,3,4 \ldots\ldots$

If the boundary condition $\Theta(\frac{H}{2}) = 0$ is employed, equation (23) becomes:

$$0 = Ee^{i(2j-1)\frac{\pi}{2}} + Ge^{-i(2j-1)\frac{\pi}{2}},$$

and since $e^{\pm j\theta} = \cos\theta \pm j \sin\theta$, equation (21) becomes:

$$0 = (E + G)\cos(2j-1)\frac{\pi}{2} + (E - G)\sin(2j-1)\frac{\pi}{2},$$

where $j = 1,2,3,4 \ldots\ldots$

Since $\cos(2j-1)\frac{\pi}{2} = 0$ and $\sin(2j-1)\frac{\pi}{2} = 1$, when $j = 1,2,3,4 \ldots\ldots$, it follows that: $E = G$.

The final solution of equation (21) is then:

$$\Theta(z) = \sum_{j=1}^{\infty} 2E \cos(2j-1)\frac{\pi z}{H}. \tag{24}$$

The general solution of equation (1) is then:

$$e_1(\rho,z,t) = \sum_{n=1}^{\infty}\sum_{j=1}^{\infty}(2E)(C)\,A_n J_o(\Lambda\rho)\cos(2j-1)\frac{\pi z}{H}\, e^{-\frac{t}{\lambda^2}}.$$

The boundary condition, $e_1(a,z,t) = 0$, implies that:

$$0 = \sum_{n=1}^{\infty}\sum_{j=1}^{\infty} D_{nj} J_o(a\Lambda)\cos\frac{(2j-1)\pi z}{H}\, e^{-\frac{t}{\lambda^2}} \tag{25}$$

and this condition necessitates that $J_o(a\Lambda) = 0$,

so that the general solution becomes:

$$e_1(\rho,z,t) = \sum_{i=1}^{\infty}\sum_{j=1}^{\infty} D_{ij} J_o(\Lambda_{ij}\rho)\cos\frac{(2j-1)\pi z}{H}\, e^{-\frac{1}{\lambda_{ij}^2}} \tag{26}$$

where D_{ij} is a constant and $\Lambda_{ij}^2 = \frac{1}{D_e} \lambda_{ij}^2 - k^2$

Only discrete values of λ_i equal to λ_{ij} will yield discrete values of Λ_{ij}, so

$$\frac{1}{\lambda_{ij}^2} = D_e (\Lambda_{ij}^2 + k^2) \quad \text{and} \quad J_o (\Lambda_{ij} a) = 0 \tag{27}$$

The final solution to equation (5) becomes:

$$e_1(\rho, z, t) = \sum_{i=1}^{\infty} \sum_{j=1}^{\infty} D_{ij} J_o(\Lambda_{ij} \rho) \cos \frac{(2j - 1)}{H} \pi z \quad e^{\frac{-t}{\lambda_{ij}^2}} \tag{28}$$

The particular solution of the partial differential equation (1) is any solution of the equation:

$$\frac{\partial e_2(\rho, z, t)}{\partial t} = D_e \nabla^2 e_2(\rho, z, t) + \sigma_1 N(\rho, z, t) \tag{29}$$

where $N(\rho, z, t) = A^2(\rho, z)\, e^{\frac{-2t}{T_m}}$. Let $N'(\rho, z, t) = \sigma_1 N(\rho, z, t)$, and equation (17) becomes:

$$\frac{\partial e_2(\rho, z, t)}{\partial t} = D_e \nabla^2 e_2(\rho, z, t) + N'(\rho, z, t). \tag{30}$$

From the theory of partial differential equations, any solution of equation (30) is a particular solution of equation (1), therefore a solution will be assumed of the form:

$$e_2(\rho, z, t) = \sum_{i=1}^{\infty} \sum_{j=1}^{\infty} \phi_{ij}(t) J_o(\Lambda_{ij} \rho) \cos \frac{(2j - 1)}{H} \pi z \quad . \tag{31}$$

$N'(\rho, z, t)$ will be expanded into an infinite Bessel-Fourier series:

$$N'(\rho,z,t) = \sum_{i=1}^{\infty}\sum_{j=1}^{\infty} N_{ij}(t)\, J_o(\Lambda_{ij}\rho)\cos\frac{(2j-1)}{H}\pi z \tag{32}$$

Substituting equations (31) and (32) into equation (30), this yields expressions of the form:

$$\frac{\partial e_2(\rho,z,t)}{\partial t} = \sum_{i=1}^{\infty}\sum_{j=1}^{\infty} J_o(\Lambda_{ij}\rho)\cos\frac{(2j-1)}{H}\pi z \quad \frac{d\phi_{ij}(t)}{\partial t} \tag{33}$$

$$D_e\nabla^2 e_2(\rho,z,t) = -D_e(\Lambda_{ij}^2 + k_j^2)^2 \sum_{i=1}^{\infty}\sum_{j=1}^{\infty} J_o(\Lambda_{ij}\rho)\cos\frac{(2j-1)}{H}\pi z\ \phi_{ij}(t) \tag{34}$$

where $\frac{1}{\lambda_{ij}^2} = D_e(\Lambda_{ij}^2 + k^j)$

$$N'(\rho,z,t) = \sum_{i=1}^{\infty}\sum_{j=1}^{\infty} N_{ij}(t)\, J_o(\Lambda_{ij}\rho)\cos\frac{(2j-1)}{H}\pi z \quad . \tag{35}$$

After substitution of these terms into equation (30) and after rearranging them, it becomes

$$\sum_{i=1}^{\infty}\sum_{j=1}^{\infty} J_o(\Lambda_{ij}\rho)\cos\frac{(2j-1)}{H}\pi z \left(\frac{d\phi_{ij}(t)}{\partial t} + \frac{1}{\lambda_{ij}^2}\phi_{ij}(t) - N_{ij}(t)\right) = 0. \tag{36}$$

One solution of equation (30) must be found and this will be the particular solution $e_2(\rho,z,t)$.

Equation (36) can be reduced to the form:

$$\frac{d\phi_{ij}(t)}{dt} + \frac{1}{\lambda_{ij}^2}\phi_{ij}(t) - N_{ij}(t) = 0 \tag{37}$$

or

$$\frac{d\phi_{ij}(t)}{dt} + \frac{1}{\lambda_{ij}^2}\,\phi_{ij}(t) = N_{ij}(t).$$

Now, $N_{ij}(t)$ must be found. Using the orthogonality properties of the Bessel and cosine functions, an expression for $N_{ij}(t)$ can be obtained. If equation (32) is multiplied on both sides by $J_o(\Lambda_{kl}\rho)$ and $\cos\frac{(2l-1)}{H}\pi z$ and integrated over the cell's dimensions, one obtains the expression:

$$\int_{-\frac{H}{2}}^{\frac{H}{2}} \int_{o}^{a} \sum_{k=1}^{\infty}\sum_{l=1}^{\infty} N(\rho,z,t)\, J_o(\Lambda_{kl}\rho)\cos\frac{(2l-1)}{H}\pi z \;\rho\, d\rho dz \qquad (38)$$

$$= \int_{-\frac{H}{2}}^{\frac{H}{2}} \int_{o}^{a} \sum_{i=1}^{\infty}\sum_{j=1}^{\infty}\sum_{k=1}^{\infty}\sum_{l=1}^{\infty} N_{ij}(t) J_o(\Lambda_{ij}\rho) J_o(\Lambda_{kl}\rho)\cos\frac{(2j-1)}{H}\pi z \cos\frac{(2l-1)}{H}\pi z\,\rho\, d\rho dz.$$

From the orthogonality properties of the functions, equation (38) reduces to zero when $k \neq i$ and $l \neq j$. The integrals in equation (38) are evaluated below when $k = i$ and $l = j$:

$$\int_{-\frac{H}{2}}^{\frac{H}{2}} \cos^2\frac{(2j-1)}{H}\pi z\, dz = \frac{H}{2} \quad \text{and} \quad \int_{o}^{a} e\,[J_o(\Lambda_{ij}\rho)]^2 d = \frac{a^2 J_1^2(\Lambda_{ij}a)}{2}$$

since $\quad [J_o(\Lambda\rho)]^2 \rho d\rho = \frac{1}{2}\,2\quad [J_o^2(\Lambda a)] + [J_1^2(\Lambda_{ij}a)]$.

Equation (38) becomes

$$\int_0^a \int_{-\frac{H}{2}}^{\frac{H}{2}} \sum_{i=1}^{\infty} \sum_{j=1}^{\infty} N'(\rho,z,t)\, J_o(\Lambda_{ij}\rho)\, \cos\frac{2j-1}{H}\pi z\ \rho d\rho dz = \frac{6^2 H J_1^2(\Lambda_j a) N_{ij}(t)}{4} \tag{39}$$

and $N_{ij}(t)$ is given by the relation:

$$N_{ij}(t) = \frac{\sum_{i=1}^{\infty}\sum_{j=1}^{\infty}\int_{-\frac{H}{2}}^{\frac{H}{2}} \int_0^a N'(\rho,z,t)\, J_o(\Lambda_{ij}\rho)\cos\frac{(2j-1)}{H}\pi z\ \rho\, d\rho dz}{\frac{a^2 H J_1^2(\Lambda_{ij}a)}{4}} \tag{40}$$

If $N'(\rho,z,t) = {}_1A^2(\rho,z)\, e^{-\frac{2t}{T_m}}$, then equation (40) becomes

$$N_{ij}(t) = \frac{e^{-\frac{2t}{T_m}} \int_{-\frac{H}{2}}^{\frac{H}{2}} \int_0^a \sum_{i=1}^{\infty} \sum_{j=1}^{\infty} A^2(\rho,z)\, J_o(\Lambda_{ij}\rho)\, \cos\frac{(2j-1)}{H}\pi z\ \rho d\rho dz}{\frac{a^2 H J_1^2(\Lambda_{ij}a)}{4}} \tag{41}$$

Let

$$A'_{ij} = \frac{\int_{-\frac{H}{2}}^{\frac{H}{2}} \int_0^a \sum_{i=1}^{\infty} \sum_{j=1}^{\infty} {}_1A^2(\rho,z)\, J_o(\Lambda_{ij}\rho)\cos\frac{(2j-1)}{H}\pi z\ \rho d\rho dz}{\frac{a^2 H J_1^2(\Lambda_{ij}a)}{4}},$$

and equation (41) can be simplified to the form:

$$N_{ij}(t) = A'_{ij} e^{-\frac{2t}{T_m}} \tag{42}$$

Upon substituting equation (42) into equation (37), the differential equation for $\phi_{ij}(t)$ becomes

$$\frac{d\phi_{ij}(t)}{dt} + \frac{1}{\lambda_{ij}^2}\phi_{ij}(t) = A'_{ij} e^{-\frac{2t}{T_m}} \tag{43}$$

The differential equation (43) has a general solution and a particular solution.

The general solution is the solution to the homogenous equation when $N_{ij}(t) = 0$. The particular solution is the solution when $N_{ij}(t) = A'_{ij} e^{\frac{-2t}{T_m}}$. The general solution is found from the equation:

$$\frac{d\phi_{ij}(t)}{dt} + \frac{1}{\lambda_{ij}^2} \phi_{ij}(t) = 0 \tag{44}$$

The solution of equation (44) is $\phi_{ij}(t) = C' e^{\frac{-t}{\lambda_{ij}^2}}$ which is similar to the solution for $e_1(\rho, z, t)$. This is the solution to the homogenous equation. The particular solution is a solution of the equation:

$$\frac{d\phi_{ij}(t)}{dt} + \frac{1}{\lambda_{ij}^2} \phi_{ij}(t) = A'_{ij} e^{\frac{-2t}{T_m}} \tag{45}$$

and can be obtained by multiplying equation (45) by $e^{\frac{+t}{\lambda_{ij}^2}}$. Equation (45) becomes

$$\frac{d\,\phi_{ij}(t)\, e^{\frac{+t}{\lambda_{ij}^2}}}{dt} = A'_{ij} e^{-t\left(\frac{2}{T_m} - \frac{t}{\lambda_{ij}^2}\right)} \tag{46}$$

which has the solution:

$$\phi_{ij}(t) = A'_{ij} e^{\frac{-t}{\lambda_{ij}^2}} - \frac{A'_{ij}}{\frac{2}{T_m} - \frac{1}{\lambda_{ij}^2}} e^{\frac{-2t}{T_m}} . \tag{47}$$

The expression for $\phi_{ij}(t)$ becomes

$$\phi_{ij}(t) = (C'_{ij} + A'_{ij}) e^{\frac{-t}{\lambda_{ij}^2}} - \frac{A_{ij}}{\frac{2}{T_m} - \frac{1}{\lambda_{ij}^2}} e^{\frac{-2t}{T_m}} \tag{48}$$

or

$$\phi_{ij}(t) = C''_{ij} \; e^{\frac{-t}{\lambda^2_{ij}}} - A''_{ij} \; e^{\frac{-2t}{T_m}}$$

where

$$C''_{ij} = C'_{ij} + A'_{ij} = \frac{A'_{ij}}{\frac{2}{T_m} - \frac{t}{\lambda^2_{ij}}}$$

where A'_{ij} is always positive. The particular solution of equation (1) becomes

$$e_2(\rho, z, t) = \sum_{i=1}^{\infty} \sum_{j=1}^{\infty} J_o(\Lambda_{ij}\rho) \cos\frac{(2j-1)}{H} \pi z \; C''_{ij} \; e^{\frac{-t}{\lambda^2_{ij}}} - A''_{ij} \; e^{\frac{-2C}{T_m}} \tag{49}$$

The overall solution, $e(\rho, z, t)$ becomes

$$e(\rho, z, t) = \sum_{i=1}^{\infty}\sum_{j=1}^{\infty} (D_{ij} + C'_{ij}) \; e^{\frac{-t}{\lambda^2_{ij}}} J_o(\Lambda_{ij}\rho) \cos\frac{(2j-1)}{H}\pi z \tag{50}$$

$$- \sum_{i=1}^{\infty}\sum_{j=1}^{\infty} A''_{ij} \; J_o(\Lambda_{ij}\rho) \cos\frac{(2j-1)}{H}\pi z \quad e^{\frac{-2t}{T_m}},$$

The solution for the electron density when simplified becomes

$$e(\rho, z, t) = \sum_{i=1}^{\infty} \sum_{j=1}^{\infty} D_{ij}(\rho, z) \, e^{\frac{-t}{\lambda^2_{ij}}} - \sum_{i=1}^{\infty} \sum_{j=1}^{\infty} M_{ij}(\rho, z) \; e^{\frac{-2t}{T_m}}, \tag{51}$$

where

$$D_{ij}(\rho, z) = (D_{ij} + C''_{ij}) \; J_o(\Lambda_{ij}\rho) \cos\frac{(2j-1)}{H} \pi z,$$

and

$$M_{ij}(\rho, z) = A''_{ij} \; (\rho, z) \; J_o(\Lambda_{ij}\rho) \cos\frac{(2j-1)}{H} \pi z \; .$$

If only the lowest mode of diffusion is considered the dominate mode, than the other diffusion modes are considered unobservable. The equation reduces to the form:

$$e(\rho,z,t) = D_{11}(\rho,z)\ e^{\frac{-t}{\lambda^2_{11}}} - M_{11}(\rho,z)\ e^{\frac{-2t}{T_m}}\ , \tag{52}$$

where $D_{11}(\rho,z)$ is the first term of the double infinite sum, $D_{ij}(\rho,z)$; $M_{11}(\rho,z)$ is also the first term of the double infinite sum, $M_{ij}(\rho,z)$; and λ_{11} is the lowest mode of the characteristic diffusion length. The quantities $M_{ij}(\rho,z)$ and $M_{11}(\rho,z)$ are given by the expressions:

$$M_{ij}(\rho,z) = A''_{ij}(\rho,z) \Big/ \frac{2}{T_m} - \frac{1}{\lambda^2_{ij}}$$

and

$$M_{11}(\rho,z) = A_{11}(\rho,z) \Big/ \frac{2}{T_m} - \frac{1}{\lambda^2_{11}}$$

$M_{11}(\rho,z)$ is a positive constant with respect to time since $A''_{11}(\rho,z)$ is positive and since the lifetime of the metastable state is smaller than the square of the lowest mode characteristic diffusion length. The characteristic diffusion length for the lowest mode is given by the expression:

$$\frac{1}{\lambda^2_{11}} = D_e\left(\Lambda^2_{11} + \frac{\pi^2}{H}\right)\ ,$$

where Λ^2_{11} is the lowest value of m such that $J_o(ma) = 0$, and H is the length of the cell and a is the radius of the experimental cell.

The rate equation for the removal of excited atoms in the i-th excited state is given by the equation:

$$\frac{\partial N_i(\rho,z,t)}{\partial t} = D_a \nabla^2 N_i(\rho,z,t) - aN_i(\rho,z,t) + \alpha e^-(\rho,z,t)\left[Hg^+\right], \tag{53}$$

and if it is assumed that $e(\rho,z,t) = \left[Hg^+\right]$, this equation becomes:

$$\frac{\partial N_i(\rho,z,t)}{\partial t} = D_a \nabla^2 N_i(\rho,z,t) - aN_i(\rho,z,t) + \alpha e^2(\rho,z,t), \tag{54}$$

where $N_i(\rho,z,t)$ is the excited atom density, $D_a \nabla^2 N_i(\rho,z,t)$ represents the diffusion loss to the walls of the cell of an excited atom, $aN_i(\rho,z,t)$ is the natural radiative decay term, and $\alpha e^2(\rho,z,t)$ represents the production of excited atoms corresponding to electron-ion recombination. The boundary conditions are

$$N_i(a,z,t) = N_i(\rho,\pm\frac{H}{2},t) = 0 \text{ and } N_i(\rho,z,o) = K(\rho,z), \tag{55}$$

It is assumed that excited atoms are destroyed through collision with the walls of the cell, and the atom density is $K(\rho,z)$ after removal of the active discharge. If equation (54) is multiplied by e^{at}, it becomes

$$e^{at}\frac{\partial N_i(\rho,z,t)}{\partial t} = D_a \nabla^2 N_i(\rho,z,t)\, e^{at} - aN_i(\rho,z,t)\, e^{at} + \alpha e^2(\rho,z,t)\, e^{at}, \tag{56}$$

and after the terms are rearranged, it becomes:

$$\frac{\partial(N_i(\rho,z,t)e^{at})}{\partial t} = D_a \nabla^2 N_i(\rho,z,t)\, e^{at} + \alpha e^2(\rho,z,t)\, e^{at}.$$

Let $U = N_i e^{at}$ and $X = \alpha e^2(\rho,z,t)e^{at}$ and equation (56) becomes:

$$\frac{\partial U(\rho,z,t)}{\partial t} = D_a \nabla^2 U(\rho,z,t) + X(\rho,z,t), \tag{57}$$

which is similar to the partial differential equation solved for the electron density.

The same procedure, that was used for the electron density equation, will be applied to solve equation (57). From the theory of partial differential equations, equation (57) has a solution of the form:

$$U(\rho,z,t) = u_1(\rho,z,t) + u_2(\rho,z,t),$$

and the solution is subject to the boundary conditions:

$$U(a,z,t) = U(\rho,\pm\frac{H}{2},t) = 0 \quad \text{and} \quad U(\rho,z,o) = g_1(\rho,z) + g_2(\rho,z).$$

$u_1(\rho,z,t)$ is the general solution to the homogenous equation and $u_2(\rho,z,t)$ is any particular solution to the partial differential equation (57). $u_1(\rho,z,t)$ is the solution of the equation:

$$\frac{\partial u_1}{\partial t} = D_a \nabla^2 u_1 , \tag{58}$$

and $u_1(\rho,z,t)$ is subject to the boundary conditions:

$$u_1(a,z,t) = u_1(\rho,\pm\frac{H}{2},t) = 0 \quad \text{and} \quad u_1(\rho,z,t) = g_1(\rho,z).$$

$u_2(\rho,z,t)$ is any solution of the equation:

$$\frac{\partial u_2}{\partial t} = D_a \nabla^2 u_2 + X \tag{59}$$

where

$$X(\rho,z,t) = \alpha e^2(\rho,z,t) e^{at} = \alpha\left(D_{11}^2(\rho,z) e^{\frac{-2t}{\lambda_{ij}^2}} - D_{11}(\rho,z) M_{11}(\rho,z) e^{-t\left(\frac{2}{T_m} + \frac{1}{\lambda_{ij}^2}\right)} + M_{11}(\rho,z)\, e^{\frac{-4t}{T_m}} \right) e^{at}$$

and $u_2(\rho,z,t)$ is subject to the boundary conditions:

$$u_2(a,z,t) = u_2(\rho,\pm\frac{H}{2},t) = 0 \quad \text{and} \quad u_2(\rho,z,o) = g_2(\rho,z)$$

In order to solve equation (58), the solution will be assumed to be of the form:

$$u_1(\rho, z, t) = X'(\rho, z)\, \Phi'(t). \tag{60}$$

When equation (60) is substituted into equation (58), this yields

$$X' \frac{d\Phi'}{dt} = \Phi' D_a \nabla^2 X'$$

$$\frac{1}{\Phi'} \frac{d\Phi'}{dt} = \frac{D_a}{X'} \nabla^2 X' = \frac{1}{\delta^2},$$

After separation of the variables, two differential equations must be solved.

These equations are

$$\frac{1}{\Phi'} \frac{d\Phi'}{dt} = -\frac{1}{\delta^2}, \tag{61}$$

and

$$\nabla^2 X' + \frac{X'}{D_a \delta^2} = 0. \tag{62}$$

The solution of equation (61) is by straightforward integration which gives

$$\Phi'(t) = \Phi'_o e^{\frac{-t}{\delta^2}} \tag{63}$$

The coordinate equation (62) may be solved by assuming a solution of the form:

$$X'(\rho, z) = R'(\rho)\, \Theta'(z) \tag{64}$$

After substituting equation (64) into equation (62), equation (62) becomes

$$\frac{1}{R'} \left(\frac{d^2 R'}{d\rho^2} + \frac{1}{\rho} \frac{dR'}{d\rho} \right) + \frac{1}{D_a \delta^2} = -\frac{1}{\Theta'} \frac{d^2\Theta'}{dz^2} = k'^2 \tag{65}$$

After separation of variables, equation (65) reduces to the two differential

equations:

$$\frac{1}{\Theta'}\frac{d^2\Theta'}{dz^2} + k'^2 = 0 \tag{66}$$

and

$$\frac{d^2R'}{d\rho^2} + \frac{1}{\rho}\frac{dR'}{d\rho} + \left(\frac{1}{D_a\delta^2} - k'^2\right)R' = 0 \tag{67}$$

Equation (67) will be solved first and Δ^2 will be substituted for the term $\frac{1}{D_a}\delta^2 - k'^2$. Equation (67) becomes

$$\frac{d^2R'}{d\rho^2} + \frac{1}{\rho}\frac{dR'}{d\rho} + \Delta^2 R' = 0\,, \tag{68}$$

which is Bessel's differential equation of the form:

$$\frac{d^2R'}{d\rho^2} + \frac{1}{\rho}\frac{dR'}{d\rho} + (m^2 - n^2)R' = 0\,, \tag{69}$$

and has possible solutions of the form:

$$R'(\rho) = A_{mn}J_n(m\rho) + B_{mn}Y_0(m\rho)\,. \tag{70}$$

From the behavior of the function $Y_0(m\rho)$, that $Y_0(m\rho) \to \infty$ as $\rho \to 0$, B_{mn} must be zero in order to have realistic solutions. In our equation, m and n are given by the relations:

$$n = 0 \quad \text{and} \quad m^2 = \Delta^2 = \frac{1}{D_a\delta^2} - k'^2\,. \tag{71}$$

Now, the most general solution will be a sum of Bessel functions, and the solution to equation (67) will be

$$R'(\rho) = \sum_{m=1}^{\infty} A_m J_o(\Delta\rho). \tag{72}$$

Equation (66), $\frac{1}{\Theta'} \frac{d^2\Theta'}{dz^2} + k'^2 = 0$, has the solution:

$$\Theta'(z) = E e^{ik'z} + G e^{-ik'z}. \tag{73}$$

Equation (73) must satisfy the boundary conditions that $\Theta\left(\frac{H}{2}\right) = \Theta\left(-\frac{H}{2}\right) = 0$, and under these boundary conditions, equation (73) becomes

$$0 = E e^{+ik'\frac{H}{2}} + G e^{-ik'\frac{H}{2}}$$

$$0 = E e^{-ik'\frac{H}{2}} + G e^{ik'\frac{H}{2}}$$

These equations are added and the result is

$$0 = E\left(e^{ik'\frac{H}{2}} + e^{-ik'\frac{H}{2}}\right) + G\left(e^{ik'\frac{H}{2}} + e^{-ik'\frac{H}{2}}\right)$$

but

$$\cos\frac{k'H}{2} = \frac{e^{ik\frac{H}{2}} + e^{ik'\frac{H}{2}}}{2}$$

so

$$0 = (E + G)\, 2\cos\frac{k'H}{2}$$

This equation will be zero if

$$\frac{k'H}{2} = \frac{(2j-1)}{H}\,\frac{\pi}{2}$$

or

$$k'_j = \frac{(2j-1)}{H}\,\pi \qquad \text{where } j = 1, 2, 3, 4 \ldots\ldots \tag{74}$$

Upon substituting equation (74) into (73), equation (73) becomes

$$\Theta(z) = E e^{\frac{i(2j-1)}{H}\pi z} + G e^{\frac{-i(2j-1)}{H}\pi z} \tag{75}$$

From the boundary condition $\Theta \frac{H}{2} = 0$, equation (73) becomes

$$0 = E e^{+i(2j-1)\frac{\pi}{2}} + F e^{-i(2j-1)\frac{\pi}{2}}$$

and from the identity, $e^{\pm i\theta} = \cos\theta \pm i \sin\theta$, equation (73) becomes

$$0 = (E + F)\cos^{(2j-1)\frac{\pi}{2}} + i(E - F)\sin^{(2j-1)\frac{\pi}{2}} \text{ where } j = 1, 2, 3 \ldots,$$

but

$$\cos^{(2j-1)\frac{\pi}{2}} = 0 \quad \text{for } j = 1, 2, 3 \ldots,$$

and

$$\sin^{(2j-1)\frac{\pi}{2}} = 1 \quad \text{for } j = 1, 2, 3 \ldots.$$

Equation (73) then becomes

$$\Theta(z) = 2E \cos\frac{(2j-1)}{H}\pi z \tag{76}$$

The solution of equation (57) becomes

$$u_1(\rho, z, t) = \sum_{n=1}^{\infty}\sum_{j=1}^{\infty} (2E)(\Phi')(A_n) J_o(\Delta_n \rho) \cos\frac{2j-1}{H}\pi z \, e^{\frac{-t}{\delta^2}} \tag{77}$$

The boundary conditions are applied and equation (77) becomes

$$u_1(a, z, t) = 0 = \sum_{n=1}^{\infty}\sum_{j=1}^{\infty} D'_{nj} J_o(\Delta_n a) \cos\frac{2j-1}{H}\pi z \; e^{\frac{-t}{\delta^2}} \tag{78}$$

where $D'_{nj} = (2E)\ (\Phi)\ (A_n)$. The fact that $u_1(a, z, t) = 0$ implies that $J_o(\Delta a) = 0$. Let Δ_{ij} be the values of Δ for which $J_o(\Delta a) = 0$, then

$$u_1(\rho, z, t) = \sum_{i=1}^{\infty}\sum_{j=1}^{\infty} D'_{ij} J_o(\Delta_{ij}\rho) \cos \frac{(2j-1)}{H}\pi z\ e^{\frac{-t}{\delta_i^2}} \tag{79}$$

where D'_{ij} is a constant, and $\Delta_{ij}^2 = \frac{1}{D_a\delta} - k'_j$. Since only discrete values of δ will yield discrete values of Δ_{ij} then

$$\frac{1}{\delta^2} = \frac{1}{\delta_{ij}^2} = D_a(\Delta_{ij}^2 + k'^2_j) \tag{80}$$

The final solution to equation (58) becomes

$$u_1(\rho, z, t) = \sum_{i=1}^{\infty}\sum_{j=1}^{\infty} D'_{ij} J_o(\Delta_{ij}) \cos\frac{(2j-1)}{H}\pi z\ e^{\frac{-t}{\delta_{ij}^2}} . \tag{81}$$

The particular solution to the partial differential equation (57) will now be obtained. It will be any solution of the equation:

$$\frac{\partial u_2}{\partial t} = D_a \nabla^2 u_2 + X , \tag{82}$$

where

$$X(\rho, z, t) = \alpha\left(D_{11}^2(\rho, z)\ e^{\frac{-2t}{\lambda_{11}^2}} - D_{11}(\rho, z)M_{11}(\rho, z)e^{-t(\frac{2}{T_m} + \frac{1}{\lambda_{ij}^2})} + M_{11}^2(\rho, z)e^{\frac{-4t}{T_m}}\right) e^{at}$$

From the theory of partial differential equations if any solution can be found to satisfy equation (82), that solution will be a particular solution to equation (57), therefore a solution of $u_2(\rho, z, t)$ is assumed to be of the form:

$$u_2(\rho, z, t) = \sum_{i=1}^{\infty} \sum_{j=1}^{\infty} J_o(\Delta_{ij}\rho) \cos \frac{(2j-1)}{H} \pi z \phi'_{ij}(t) \tag{83}$$

$X(\rho, z, t)$ is now expanded as an infinite Bessel-Fourier series:

$$X(\rho, z, t) = \sum_{i=1}^{\infty} \sum_{j=1}^{\infty} X_{ij}(t) J_o(\Delta_{ij}\rho) \cos \frac{(2j-1)}{H} \pi z. \tag{84}$$

On substituting equations (83) and (84) into (82), the separate terms of equation (82) reduce to the form:

$$\frac{\partial u_2}{\partial t}(\rho, z, t) = \sum_{i=1}^{\infty} \sum_{j=1}^{\infty} J_o(\Delta_{ij}\rho) \cos \frac{(2j-1)}{H} \pi z \frac{d\phi_{ij}(t)}{dt} \tag{85}$$

$$D_a \nabla^2 u_2(\rho, z, t) = -D_a(\Delta_{ij}^2 + k'^2) \sum_{i=1}^{\infty} \sum_{j=1}^{\infty} J_o(\Delta_{ij}\rho) \cos \frac{(2j-1)}{H} \pi z \phi_{ij}(t) \tag{86}$$

and

$$X(\rho, z, t) = \sum_{i=1}^{\infty} \sum_{j=1}^{\infty} X_{ij}(t) J_o(\Delta_{ij}\rho) \cos \frac{(2j-1)}{H} \pi z \tag{87}$$

where $$\frac{1}{\delta_{ij}^2} = D_a(\Delta_{ij}^2 + k'^2)$$

After substituting equation (85), (86) and (87) into equation (82) and rearranging terms, equation (82) becomes

$$\sum_{i=1}^{\infty} \sum_{j=1}^{\infty} J_o(\Delta_{ij}\rho) \cos \frac{(2j-1)}{H} \pi z \left(\frac{d\phi'_{ij}}{dt} + \frac{1}{\delta_{ij}^2} \phi'_{ij}(t) - X_{ij}(t) \right) = 0. \tag{88}$$

Equation (88) has a solution only if:

$$\frac{d\phi'_{ij}(t)}{dt} + \frac{1}{\delta^2_{ij}}\phi'_{ij}(t) - X_{ij}(t) = 0 \qquad (89)$$

or

$$\frac{d\phi'_{ij}(t)}{dt} + \frac{1}{\delta^2_{ij}}\phi'(t) = X_{ij}(t) \; .$$

Now, $X_{ij}(t)$ must be found. Using the orthogonality properties of the Bessel functions and cosine functions, $X_{ij}(t)$ can be found. If equation (82) is multiplied by $J_o(\Delta_{kl}\rho)$and $\cos\frac{(2l-1)}{H}\pi z$ on both sides of the equation and integrated over the dimensions of the cell, it yields

$$\int_{-\frac{H}{2}}^{\frac{H}{2}}\int_{o}^{a} \sum_{k=1}^{\infty}\sum_{l=1}^{\infty} X'(\rho, z, t) J_o(\Delta_{kl}\rho) \cos\frac{(2l-1)}{H}\pi z \; \rho\, d\rho\, dz \qquad (90)$$

$$= \int_{-\frac{H}{2}}^{\frac{H}{2}}\int_{o}^{a} \sum_{i=1}^{\infty}\sum_{j=1}^{\infty}\sum_{k=1}^{\infty}\sum_{l=1}^{\infty} X_{ij}(t) J_o(\Delta_{ij}\rho) J_o(\Delta_{kl}\rho)\cos\frac{(2j-1)}{H}\pi z \cos\frac{(2l-1)}{H}\pi z \rho \, d\rho\, dz$$

From the orthogonality properties of the functions, equation (90) is equal to zero if $k \neq i$ and $l \neq j$, and if $k = i$ and $l = j$, then $X_{ij}(t)$ becomes

$$X_{ij}(t) = \int_{-\frac{H}{2}}^{\frac{H}{2}}\int_{o}^{a} \sum_{i=1}^{\infty}\sum_{j=1}^{\infty} \frac{X(\rho, z, t) J_o(\Delta_{ij}\rho)\cos\frac{(2j-1)}{H}\pi z \; \rho\, d\rho\, dz}{\frac{a^2 H J_1^2(\Delta_{ij} a)}{4}} \; . \qquad (91)$$

$$\text{If } X(\rho, z, t) = \alpha \; D_{11}^2(\rho, z)\, e^{-\frac{2t}{\lambda_{11}^2}} - D_{11}(\rho, z) M_{11}(\rho, z)\, e^{-(\frac{2}{T_m} + \frac{1}{\lambda_{11}})t} + M_{11}(\rho, z)\, e^{-\frac{4t}{T_m}}\, e^{at},$$

then

$$X_{ij}(t) = A'_{ij}\, e^{-\frac{2t}{\lambda_{11}^2}} - B'_{ij}\, e^{-t(\frac{2}{T_m} + \lambda_{11})} + C'_{ij}\, e^{-\frac{4t}{T_m}}\, e^{at},$$

where

$$A'_{ij} = \frac{\sum_{i=1}^{\infty}\sum_{j=1}^{\infty} \int_{-\frac{H}{2}}^{\frac{H}{2}} \int_{0}^{a} \alpha D_{11}^2(\rho, z) J_o(\Delta_{ij}\rho) \cos\frac{(2j-1)}{H}\pi z \; \rho\, d\rho\, dz}{\frac{a^2 H J_1^2(\Delta_{ij} a)}{4}}$$

$$B'_{ij} = \frac{\sum_{i=1}^{\infty}\sum_{j=1}^{\infty} \int_{-\frac{H}{2}}^{\frac{H}{2}} \int_{0}^{a} \alpha D_{11}(\rho, z) M_{11}(\rho, z) J_o(\Delta_{ij}\rho) \cos\frac{(2j-1)}{H}\pi z \; \rho\, d\rho\, dz}{\frac{a H J_1^2(\Delta_{ij} a)}{4}}$$

and

$$C'_{ij} = \frac{\sum_{i=1}^{\infty}\sum_{j=1}^{\infty} \int_{-\frac{H}{2}}^{\frac{H}{2}} \int_{0}^{a} \alpha M_{11}^2(\rho, z) J_o(\Delta_{ij}\rho) \cos\frac{2j-1}{H}\pi z \; \rho\, d\rho\, dz}{\frac{a^2 H J_1(\Delta_{ij} a)}{4}}$$

The differential equation (89) becomes

$$\frac{d\phi'_{ij}(t)}{dt} + \frac{1}{\delta^2_{ij}}\phi'_{ij}(t) = e^{a} \cdot A'_{ij} e^{\frac{-2t}{\lambda^2_{11}}} - B'_{ij} e^{-(\frac{2}{T_m} + \frac{1}{\lambda^2_{11}})} + C'_{ij} e^{\frac{-4t}{T_m}} \quad (92)$$

Equation (92) has a general solution an a particular solution. The general solution occurs when $n'_{ij}(t) = 0$, and the particular solution occurs when

$$n_{ij}(t) = e^{a} \quad A'_{ij} e^{\frac{-2t}{\lambda^2_{11}}} - B' e^{-t(\frac{2}{T_m} + \frac{1}{\lambda^2_{11}})} + C'_{ij} e^{\frac{-4t}{T_m}}$$

The general solution is the solution of the differential equation:

$$\frac{d\phi'_{ij}(t)}{dt} + \frac{1}{\delta^2_{ij}}\phi'_{ij}(t) = 0 \quad (93)$$

which is $\phi'_{ij}(t) = \Phi'_o e^{\frac{-t}{\delta^2_{ij}}}$, and this solution is similar to the solution for $u_1(\rho, z, t)$. The particular solution of equation (92) is

$$\phi'_{ij}(t) = e^{a} \quad A'_{ij} e^{\frac{-2t}{\lambda^2_{11}}} - B'_{ij} e^{-t(\frac{2}{T_m} + \frac{1}{\lambda^2_{11}})} + C_{ij} e^{\frac{-4t}{T_m}} + G_{ij} e^{\frac{-t}{\delta^2_{ij}}}$$

where

$$A''_{ij} = \frac{A''_{ij}}{a + \frac{1}{\delta^2_{ij}} - \frac{2}{\lambda^2_{11}}} \quad B''_{ij} = \frac{B''_{ij}}{a + \frac{1}{\delta^2_{ij}} - \frac{4}{T_m} - \frac{1}{\lambda^2_{11}}}, \text{ and } C''_{ij} = \frac{C''_{ij}}{a + \frac{1}{\delta^2_{ij}} - \frac{4}{T_m}} \quad (94)$$

Equation (92) has the solution:

$$\phi'_{ij}(t) = \Phi''_o e^{\frac{-t}{\delta^2_{ij}}} + e^{a} \quad A''_{ij} e^{\frac{-2t}{\lambda^2_{11}}} - B''_{ij} e^{-t(\frac{2}{T_m} + \frac{1}{\lambda^2_{11}})} + C''_{ij} e^{\frac{-4t}{T_m}} \quad (95)$$

The particular solution to the partial differential equation (57) becomes

$$u_2(\rho,z,t) = \sum_{i=1}^{\infty}\sum_{j=1}^{\infty} J_o(\Delta_{ij}\rho)\cos\frac{2j-1}{H}\pi z \; \Phi_o'' e^{-\frac{t}{\delta_{ij}^2}} \tag{96}$$

$$+ e^{a} \; A_{ij}'' e^{-\frac{2t}{\lambda_{11}^2}} - B_{ij}'' e^{-t\left(\frac{2}{T_m}+\frac{1}{\lambda_{11}^2}\right)} + C_{ij}'' e^{-\frac{4t}{T_m}}$$

The final solution for the rate equation for the atom density is

$$u(\rho,z,t) = u_1(\rho,z,t) + u_2(\rho,z,t) \tag{97}$$

which has the form:

$$u(\rho,z,t) = \sum_{i=1}^{\infty}\sum_{j=1}^{\infty} (D_{ij}' + \Phi_o'') e^{-\frac{t}{\delta_{ij}^2}} J_o(\Delta_{ij}\rho)\cos\frac{2j-1}{H}\pi z \tag{98}$$

$$+ \sum_{i=1}^{\infty}\sum_{j=1}^{\infty} e^{at} A_{ij}' e^{-\frac{2t}{\lambda_{11}^2}} - B_{ij}' e^{-t\left(\frac{2}{T_m}+\frac{1}{\lambda_{11}^2}\right)} + C_{ij}' e^{-\frac{4t}{T_m}} J_o(\Delta_{ij})$$

$$\cos\frac{(2j-1)\pi z}{H} \; .$$

and the equation reduces to the form:

$$u(\rho,z,t) = F_{ij}(\rho,z)\, e^{-\frac{t}{\delta_{ij}^2}} + e^{at} \; A_{ij}(\rho,z)\, e^{-\frac{2t}{\lambda_{11}^2}} + C_{ij}(\rho,z)\, e^{-\frac{4t}{T_m}} - B_{ij}(\rho,z)$$

$$e^{-t\left(\frac{2}{T_m}+\frac{1}{\lambda_{11}^2}\right)} \tag{99}$$

where

$$F_{ij}(\rho,z) = \sum_{i=1}^{\infty}\sum_{j=1}^{\infty} (D_{ij} + \Phi_o')\, J_o(\Delta_{ij}\rho)\cos\frac{2j-1}{H}\pi z \; ,$$

$$A_{ij}(\rho,z) = \sum_{i=1}^{\infty}\sum_{j=1}^{\infty} A''_{ij} J_o(\Delta_{ij}\rho)\cos\frac{2j-1}{H}\pi z,\quad B_{ij}(\rho,z) = \sum_{i=1}^{\infty}\sum_{j=1}^{\infty} B''_{ij} J_o(\Delta_{ij}\rho)$$

$$\cos\frac{2j-1}{H}\pi z, \text{ and } C_{ij}(\rho,z) = \sum_{i=1}^{\infty}\sum_{j=1}^{\infty} C''_{ij} J_o(\Delta_{ij}\rho)\cos\frac{2j-1}{H}\pi z.$$

From the transformation equation $U(\rho,z,t) = N_i(\rho,z,t)\, e^{at}$, the expression for the excited atom density becomes

$$N_i(\rho,z,t) = F_{ij}(\rho,z)\, e^{-t\left(\frac{1}{\delta_{ij}^2}+a\right)} + A_{ij}(\rho,z)\, e^{\frac{-2t}{\lambda_{11}^2}} + C_{ij}(\rho,z)\, e^{\frac{-4t}{T_m}} - B_{ij}\, e^{-t\left(\frac{2}{T_m}+\frac{1}{\lambda_{11}^2}\right)}. \tag{100}$$

It will be assumed that only the lowest mode of atom diffusion dominates, then equation (100) reduces to

$$N_i(\rho,z,t) = F_{11}(\rho,z)\, e^{-t\left(\frac{1}{\delta_{11}^2}+a\right)} + A_{11}(\rho,z)\, e^{-\frac{2t}{\lambda_{11}^2}} C_{11}(\rho,z)\, e^{\frac{-4t}{T_m}} - B_{11}(\rho,z)\, e^{-t\left(\frac{2}{T_m}+\frac{1}{\lambda_{11}^2}\right)}.$$

where $F_{11}(\rho,z)$, $C_{11}(\rho,z)$, $A_{11}(\rho,z)$ and $B_{11}(\rho,z)$ are all positive first terms of the infinite sum of the coefficients of equation (100). These terms can be observed to be positive for the lowest diffusion mode from equation (94) since a is the largest and dominate term--in order of magnitude $a > \frac{4}{T_m} > \frac{1}{\lambda_{11}^2} > \frac{1}{\delta_{11}^2}$.

The rate equation governing the removal of 6^3P_2 metastable atoms from the afterglow is

$$\frac{\partial M(\rho, z, t)}{dt} = D_m \nabla^2 M(\rho, z, t) - \sigma_1 M^2(\rho, z, t) \tag{101}$$

where $M(\rho, z, t)$ represents the metastable atom density, $D_m \nabla^2 M(\rho, z, t)$ represents the loss of atoms by diffusion to the walls of the cell, and σM^2 (ρ, z, t) represents the loss of metastable atoms by collisions with similar atoms to produce mercury ions and electrons. By neglecting diffusion, equation (100) becomes

$$\frac{dM(\rho, z, t)}{dt} = -\sigma_1 M^2(\rho, z, t) , \tag{102}$$

which has a solution of the form:

$$M(\rho, z, t) = \frac{A(\rho, z)}{1 + A(\rho, z)\, \sigma_1 t} \qquad A(\rho, z)\, e^{-A(\rho z)\, \sigma_1 t} \qquad A(\rho, z)\, e^{\frac{-t}{T_m}} \tag{103}$$

under the boundary conditions:

$$M(\rho, z, 0) = A(\rho, z) \qquad \text{and} \qquad \sigma_1 A(\rho, z) = \frac{1}{T_m}$$

where $A(\rho, z)$ is the metastable atom concentration at the end of the active discharge.